

Optimal scaling laws in learning hierarchical multi-index models

Leonardo Defilippis¹, Florent Krzakala², Bruno Loureiro¹, and Antoine Maillard^{1,3}

¹Departement d’Informatique, École Normale Supérieure, PSL & CNRS

²Information, Learning and Physics Laboratory, École Polytechnique Fédérale de Lausanne (EPFL)

³INRIA Paris

Abstract

In this work, we provide a sharp theory of scaling laws for two-layer neural networks trained on a class of *hierarchical multi-index* targets, in a genuinely representation-limited regime. We derive exact information-theoretic scaling laws for subspace recovery and prediction error, revealing how the hierarchical features of the target are sequentially learned through a cascade of phase transitions. We further show that these optimal rates are achieved by a simple, target-agnostic spectral estimator, which can be interpreted as the small learning-rate limit of gradient descent on the first-layer weights. Once an adapted representation is identified, the readout can be learned statistically optimally, using an efficient procedure. As a consequence, we provide a unified and rigorous explanation of scaling laws, plateau phenomena, and spectral structure in shallow neural networks trained on such hierarchical targets.

1 Introduction

Despite the staggering practical success of neural networks, we still lack a predictive theory answering a deceptively simple question: given a structured learning problem, *how does the network adapts to the task, in what order are the relevant features in the data learned, and how these translate in statistical efficiency?* This question sits at the intersection of three active lines of research. First, the empirical observation of *neural scaling laws* (Kaplan et al., 2020; Brown et al., 2020; Hoffmann et al., 2022) suggest that the performance of large models scale as a power-law in the training resources, yet—with few exceptions—our mathematical understanding of this relationship remains largely confined to linear models or networks in the lazy regime. Second, recent literature of the training dynamics of neural networks increasingly suggest that feature learning is not a smooth process, but are associated to long *plateaus and abrupt transitions* in the risk, with features (or *concepts* in this context) appearing sequentially rather than all at once Saxe et al. (2014); Wei et al. (2022); Schaeffer et al. (2023).

Third, empirical analyses of trained networks have uncovered robust regularities in how the learned representations manifest in the trained network weights, such as in their spectral structure, but without a first-principles explanation of *why* particular features are preferred or *when* they should emerge (Martin and Mahoney, 2021; Wang et al., 2023; Thamm et al., 2024).

This paper provides an end-to-end answer to these questions in a mathematically tractable—yet genuinely feature learning—setting of a two-layer neural network trained on *hierarchical multi-index* data, a class of structured supervised learning tasks where the target function depends on a hierarchical combination of functions of the covariates Ren et al. (2025); Ben Arous et al. (2025); Defilippis et al. (2025b). Here, hierarchical denote the fact that the direction are *ordered*, in the sense that their relative importance decay as a power-law with their index number. This leads to a quasi-sparsity of the target representation, with ordered hierarchy of feature strengths as is classical in signal processing Mallat (1999); Donoho (2006).

In this task, learning is fundamentally *representation-limited*: the labels $y = g(\mathbf{W}_* \mathbf{x})$ depend on a low-dimensional but unknown subspace $\text{span}(\mathbf{W}_*) \subset \mathbb{R}^d$ of the input space $\mathbf{x} \in \mathbb{R}^d$, and generalization hinges on discovering this subspace as well as possible from the data. Our goal is to turn this qualitative picture into sharp, quantitative predictions. More precisely, our **main contributions** are:

- (i) **Optimal Bayes rates for feature recovery.** We derive the exact information-theoretic limits for recovering the features subspace $\text{span}(\mathbf{W}_*)$ from $n = \Theta(d)$ samples. Further, we precisely characterize the associated optimal mean-squared error rates (a.k.a. *scaling laws*), unveiling the presence of cross-overs and plateaus regions that translate a fundamental trade-off between data-scarce and model-limited regions, depending on the hardness of the underlying hierarchical structure. Interestingly, these rates coincide with the minimax bounds for quasi-sparse recovery achieved by the LASSO [Raskutti et al. \(2011\)](#), and with previously conjectured results for shallow networks with quadratic activation [Defilippis et al. \(2024\)](#). Our analysis shows that these scalings are in fact universal for a broad class of hierarchical multi-index targets, well beyond the quadratic setting.
- (ii) **A matching spectral algorithm and sequential feature emergence.** We introduce a simple, *target-agnostic* spectral estimator that provably achieves the Bayes-optimal rates derived above. This estimator can be either interpreted as a spectral method applied to the network, or as the small-learning-rate limit of gradient descent on a suitably regularized loss, via the Hessian of a modified objective. As a consequence, gradient-based training is shown to recover the signal subspace optimally, provided it is properly tuned. Moreover, the recovery proceeds sequentially: the i -th direction in the hierarchy becomes detectable at a sample complexity $n_i = \Theta(i^{2\gamma}d)$ —where γ is the exponent controlling the hierarchy— leading to a cascade of sharp phase transitions. This produces plateaus and abrupt drops in the prediction error, providing a theoretical account of the progressive emergence of features observed empirically in neural networks.
- (iii) **Learnability of the target function by neural networks.** Once the features/concepts subspace is identified, we show that learning the second-layer (readout) weights incurs no additional statistical bottleneck: the resulting prediction error matches the Bayes-optimal rate for subspace recovery. Crucially, this two-stage procedure succeeds because the spectral subspace estimator is fully agnostic to the target function and does not require any prior knowledge of its structure or tuning to its decay profile. We prove that this two-stage mechanism—optimal representation discovery followed by efficient readout estimation—applies in the noisy and regularized setting, and to a wide class of multi-index targets.

Together, these results show that representation learning proceeds through a sequence of sharp phase transitions as the number of samples increases. New directions in the signal subspace emerge one after another, leading to plateaus and abrupt drops in the prediction error. This sequential emergence (to borrow the terminology of [Wei et al. \(2022\)](#); [Schaeffer et al. \(2023\)](#)) of features provides a precise theoretical underpinning for the empirically observed phenomenon of progressive concept learning in neural networks. Strikingly, the resulting phenomenology closely mirrors that recently uncovered for diagonal and quadratic neural networks using heuristic tools from statistical physics, where progressive feature emergence and distinct scaling regimes were observed ([Defilippis et al., 2025b](#)). Our contribution is to place this picture on firm theoretical ground and to substantially generalize it to a broader and more realistic class of models and targets.

Further related works — Most theoretical work on neural scaling laws focus on effectively linear models, such as kernel methods and random features, where the generalization behavior can be characterized through spectral properties of fixed representations ([Caponnetto and De Vito, 2007](#); [Spigler et al., 2020](#); [Cui et al., 2021; 2023](#); [Defilippis et al., 2024](#); [Atanasov et al., 2024](#); [Bahri et al., 2024](#); [Maloney et al., 2022](#); [Paquette et al., 2024](#); [Kunstner and Bach, 2025](#); [Bordelon et al., 2020](#)). Exceptions have focused either in the joint-training of both layers for linear networks [Bordelon et al. \(2024; 2025\)](#); [Worschech and Rosenow \(2024\)](#) or non-linear settings with fixed-features [Wortsman and Loureiro \(2025\)](#); [Worschech and Rosenow \(2024\)](#); [Braun et al. \(2025\)](#). A central difference is that these works introduce scaling through the covariate distribution, while in our work it is induced by the hierarchical nature of the task. Moreover, our work departs from this literature by addressing scaling laws in a genuinely non-linear, feature-learning regime.

Closer to us are a recent line of work analyzing two-layer networks with structured first-layer weights and hierarchical multi-index target ([Ren et al., 2025](#); [Ben Arous et al., 2025](#); [Defilippis et al., 2025b](#)). In particular, [Ren et al. \(2025\)](#); [Ben Arous et al. \(2025\)](#) studied one-pass SGD in this setting, with [Ben Arous et al. \(2025\)](#) focusing on the case of a quadratic neural network architecture. The main difference with this work is that we analyze full-batch ERM, characterizing the optimal scaling laws and showing that they can be achieved computationally by a gradient-descent like algorithm, thus providing a fundamental benchmark for the SGD rates in these works.

Complementary, Defilippis et al. (2025b) derived rates for ERM in quadratic neural networks trained on quadratic targets, building on earlier work by Erba et al. (2025) (see also Maillard et al. (2024); Xu et al. (2025); Martin et al. (2026)). Our results show that the rates from Defilippis et al. (2025b) are universal a large class of target functions (any generative exponent two functions in the language of Damian et al. (2024)), closing a gap between the purely quadratic setting and general hierarchical multi-index targets. The key underlying these universal scaling laws is the combination *quasi-sparsity* of the target representation, encoded by a heavy-tailed spectrum that induces an ordered hierarchy of feature strengths (Mallat, 1999; Donoho, 2006), and an implicit *rank-sparsity* bias, leading to LASSO-like behavior (Raskutti et al., 2011).

On a technical level, our work builds on the toolbox of approximate message passing (AMP) and its associated state evolution (Bayati and Montanari, 2011; Donoho et al., 2013; Javanmard and Montanari, 2013; Berthier et al., 2020; Zou and Yang, 2022; Feng et al., 2022; Gerbelot and Berthier, 2023; Dudeja et al., 2023; Erba et al., 2025). In particular, our results leverage the connection between AMP and Bayes-optimal estimation for single- Barbier et al. (2019) and multi-index Aubin et al. (2018); Troiani et al. (2025) models. Similarly, we build up on the literature on optimal spectral methods derived from AMP for single- (Mondelli and Montanari, 2019; Lu and Li, 2020; Maillard et al., 2022; Damian et al., 2024) and multi-index Kovačević et al. (2025); Defilippis et al. (2025a) functions.

2 Setting

Consider a supervised regression problem with training data $\mathcal{D} = \{(\mathbf{x}_i, y_i) \in \mathbb{R}^{d+1} : i \in [n]\}$, which we assumed were drawn i.i.d. from a joint distribution over \mathbb{R}^{d+1} . Recall that the goal in regression is to learn a target function $f_\star(\mathbf{x}) = \mathbb{E}[y|\mathbf{x}]$ from the training data \mathcal{D} . In the following, we will be interested in particular structured tasks where the dependence of the target f_\star on the covariates $\mathbf{x} \in \mathbb{R}^d$ is given by a hierarchical combination of low-dimensional subtasks. Mathematically, this is formalized by *hierarchical multi-index models*.

Definition 2.1 (Hierarchical multi-index model). Let $\mathbf{W}_\star = (\mathbf{w}_k^\star \in \mathbb{R}^d)_{k \in [m_\star]}$ denote a family of m_\star orthogonal vectors of norm $\|\mathbf{w}_k^\star\|^2 = d$. A *hierarchical multi-index* target is defined as

$$f_\star(\mathbf{x}) = \sum_{k=1}^{m_\star} a_k^\star g_k(\langle \mathbf{w}_k^\star, \mathbf{x} \rangle), \quad (1)$$

where $a_1^\star > a_2^\star > \dots > a_{m_\star}^\star$ satisfy $\sum_{k=1}^{m_\star} (a_k^\star)^2 = 1$ and $g_k : \mathbb{R} \rightarrow \mathbb{R}$. Moreover, we say f_\star is a *scale-free* hierarchical multi-index model if $a_k^\star = \Theta(k^{-\gamma})$ for some $\gamma > 0$.

A few remarks are in order.

- As the name suggests, hierarchical multi-index models can be seen as a sum of m_\star effectively one-dimensional tasks $g_k(z_k)$, with decreasing weight a_k^\star .
- More generally, multi-index models are functions of the type $f_\star(\mathbf{x}) = g(\mathbf{W}_\star \mathbf{x})$, where $g : \mathbb{R}^{m_\star} \rightarrow \mathbb{R}$ is known as the *link function* and

$$\mathbf{z} = \mathbf{W}_\star \mathbf{x} \in \mathbb{R}^{m_\star} \quad (2)$$

are known as the *indices*. They have been widely studied as statistical models for regression in the statistics literature Li (1991); Yuan (2011); Babichev and Bach (2018).

- More recently, multi-index models have gained in popularity in the machine learning theory literature as generative models for data, where they have been used to prove feature learning separation results for neural networks Damian et al. (2022); Abbe et al. (2023); Dandi et al. (2024).
- Scale-free hierarchical multi-index models were considered recently in Ren et al. (2025); Ben Arous et al. (2025); Defilippis et al. (2025b). Note that when $\gamma > 1/2$, the target is *quasi-sparse* in the index basis (Mallat, 1999; Donoho, 2006). This makes the model a suitable framework for investigating feature learning in neural networks, which are known to exhibit an implicit bias towards sparse estimators Gunasekar et al. (2017); Soudry et al. (2018); Andriushchenko et al. (2023).

- In scale-free hierarchical multi-index models with $\gamma < 1/2$, the coefficients must scale as $a_k^* = \Theta(k^{-\gamma} m_*^{\gamma-1/2})$ to guarantee the boundedness of the labels.

Definition 2.2. The training data $\mathcal{D} = \{(\mathbf{x}_i, y_i) \in \mathbb{R}^{d+1} : i \in [n]\}$ is drawn i.i.d. from a scale-free hierarchical multi-index model $f_*(\mathbf{x})$ as in Def. 2.1, in particular

$$y_i = f_*(\mathbf{x}_i) + \sqrt{\Delta} \xi_i \quad (3)$$

where $\mathbf{x}_i \sim \mathcal{N}(0, 1/d \mathbf{I}_d)$, $\Delta > 0$ is the noise variance and $\xi_i \sim \mathcal{N}(0, 1)$.

Moreover, our results depend on the following additional assumption on the link function.

Assumption 2.3. For each index $k \in [m_*]$, g_k is an even function. Moreover, for $z \sim \mathcal{N}(0, 1)$, for some constants $b, C, D > 0$, independent of k, n, d, α, m_* ,

$$|g_k(z)| \leq C(1 + |z|^b), \quad (4)$$

$$D < \mathbb{E}_z[g_k^2(z)] < C, \quad D < |\mathbb{E}_z[g_k''(z)]| < C. \quad (5)$$

Remark 2.4. The parity assumption on g_k ensures that learning $\text{span}(\mathbf{W}_*)$ is *non-trivial*, by ruling out linear correlations that would allow recovery at arbitrarily small sample complexity. Indeed, given \mathbf{z} as in eq. (2) and y as in eq. 3, when $\mathbb{E}[\mathbf{z} | y] = 0$ a.s.—which holds here by parity—no efficient algorithm can even weakly recover $\text{span}(\mathbf{W}_*)$ below the critical threshold

$$\alpha_c := \left(\sup_{\mathbf{M} \in \mathbb{S}_{m_*}^+, \|\mathbf{M}\|_F=1} \|\mathbb{E}_y \mathbf{G}(y) \mathbf{M} \mathbf{G}(y)\|_F \right)^{-1}, \quad (6)$$

with $\mathbf{G}(y) := \mathbb{E}[\mathbf{z} \mathbf{z}^\top | Y = y]$ [Barbier et al. \(2019\)](#); [Mondelli and Montanari \(2019\)](#); [Lu and Li \(2020\)](#); [Damian et al. \(2024\)](#); [Troiani et al. \(2025\)](#).

The condition on $\mathbb{E}_z[g_k^2(z)]$ controls the label variance, while the lower bound on $\mathbb{E}_z[g_k''(z)]$ ensures detectability in the proportional regime $n = \Theta(d)$ (equivalently, a generative exponent equal to 2), so that the relative difficulty of each index is governed solely by the decay of a_k^* . ¹

Hierarchical multi-index models with generative exponent equal to 2 includes the vast majority of cases of interest, while the class of models with exponent larger than 2 mostly includes fine-tuned examples [Barbier et al. \(2017\)](#); [Damian et al. \(2024\)](#).

Our key goals in the following are twofold: (i) to characterize what are the best achievable rates (a.k.a. scaling laws) in recovering concepts and features for this class of hierarchical tasks; (ii) to show that out-of-the box models such as neural networks can learn efficiently the features, and the entire functions as well, with those optimal scaling rates.

In order to quantify the recovery of each individual index, or concept, we define following metric.

Definition 2.5 (Matrix-MSE). Let $\mathbf{w}_k^* \in \mathbb{S}^{d-1}(\sqrt{d})$ denote one of the target indices $k \in [d]$. We define the matrix-MSE associated to a predictor $\mathbf{w} \in \mathbb{R}^d$ as:

$$\text{mse}_k(\mathbf{w}) := \frac{1}{d^2} \mathbb{E} [\|\mathbf{w} \mathbf{w}^\top - \mathbf{w}_k^* \mathbf{w}_k^{*\top}\|_F^2]. \quad (7)$$

Additionally, we characterize the *weak recovery* transition for the index k , *i.e.* the minimum number of samples required by an estimator to correlate non-trivially with a specific concept.

Definition 2.6 (k -critical threshold). Given an estimator $\hat{\mathbf{w}}_k \in \mathbb{R}^d$ of the signal direction \mathbf{w}_k^* (*i.e.* a measurable function of the training data \mathbf{X}, \mathbf{y}), the k -critical threshold is defined as the minimum sample complexity such that the estimator exhibits a finite overlap with $\mathbf{w}_{*,k}$, namely

$$\inf \{\alpha > 0 : d^{-1} |\langle \hat{\mathbf{w}}_k, \mathbf{w}_{*,k} \rangle| = \Theta_d(1)\}. \quad (8)$$

¹Our analysis can be easily adapted to the less restrictive assumption that there exists an integer $\beta \geq 1$ such that $D < |\mathbb{E}_Z[g_k^\beta(Z)(Z^2 - 1)]| < C$. This would result in a simple modification of the scaling laws and not affect the overall message of the present manuscript.

The recovery of $\text{span}(\mathbf{W}^*)$ is assessed by the sum of the squared errors for each individual direction, weighted by the contribution of each concept to the target variance.

Definition 2.7 (Weighted MSE). Let $\mathbf{W} \in \mathbb{R}^{m_* \times d}$. We define the weighted mean-squared error as

$$\text{MSE}_\gamma(\mathbf{W}) := \sum_{k \in K} (a_k^*)^2 \text{mse}_k(\mathbf{w}_k). \quad (9)$$

For the second goal — showing that neural networks can efficiently learn f_* — we will focus on two-layer neural networks:

$$f(\mathbf{x}; \Theta) := \mathbf{a}^\top \sigma(\mathbf{W}\mathbf{x} + \mathbf{b}), \quad (10)$$

with weights $\Theta := (\mathbf{a} \in \mathbb{R}^p, \mathbf{W} \in \mathbb{R}^{p \times d})$ and a generic activation function $\sigma : \mathbb{R} \rightarrow \mathbb{R}$. As we shall see, two-layer neural networks can agnostically learn with respect to the model, i.e. without knowledge of the individual tasks g_k nor the details in Def. 2.1. We quantify the generalization capacity of this model through its excess risk

$$R(\Theta) = \mathbb{E} \left[(f_*(\mathbf{x}) - f(\mathbf{x}; \Theta))^2 \right]. \quad (11)$$

3 Main results

We now discuss our main contributions, which are threefold. First, we will derive the information-theoretical optimal reconstruction error for the class of scale-free hierarchical multi-index models introduced in Theorem 2.2, as quantified by the weighted reconstruction error in Equation (9). This result will serve as a fundamental benchmark on the difficulty of subspace recovery for a given $\gamma > 0$. Second, we will construct a spectral estimator for subspace recovery, and will prove that this algorithm achieves the aforementioned optimal reconstruction error. Finally, we turn our attention to two-layer neural networks, proving that a two-step training procedure also achieves the optimal scaling laws for the excess risk.

3.1 Bayes-optimal rates for feature recovery

As a first result, we characterize the information-theoretic limits for the recovery of the subspace $\text{span}(\mathbf{W}_*)$ in terms of the decay of the target coefficients \mathbf{a}^* , the sample complexity α and the subspace dimension m_* .

Definition 3.1 (Optimal MSE). Let $\mathcal{D} = (\mathbf{X}, \mathbf{y})$ be drawn as in def. 2.2. Then, the optimal (weighted) mean-square error is achieved by the posterior average:

$$\text{MMSE}_\gamma := \sum_{k=1}^{m_*} \frac{(a_k^*)^2}{d^2} \mathbb{E} \left[\|\mathbb{E}[\mathbf{w}_k \mathbf{w}_k^\top | \mathcal{D}] - \mathbf{w}_k^* \mathbf{w}_k^{*\top}\|_F^2 \right]$$

By definition, MMSE_γ is a lower-bound for the smallest achievable weighted mean-squared error $\text{MSE}_\gamma(\hat{\mathbf{W}})$ by any estimator $\hat{\mathbf{W}}$ that is a function of the dataset \mathcal{D} . Our first main result quantifies precisely the rates of MMSE_γ as $\alpha \gg 1$, which by construction define the optimal scaling laws for subspace reconstruction in the class of scale-free hierarchical multi-index models.

Theorem 3.2 (Optimal scaling-laws). *In the setting of Definitions 2.1, 2.2, under Assumption 2.3, for $\alpha, m_* \gg 1$, the Bayes-optimal mean-squared error satisfies*

$$\text{MMSE}_\gamma = \Theta_{\alpha, m_*} \begin{cases} \alpha^{-1+1/2\gamma}, & \gamma > 1/2, \alpha \ll m_*^{2\gamma}, \\ m_*/\alpha, & \gamma > 1/2, m_*^{2\gamma} \ll \alpha, \\ 1, & \gamma < 1/2, \alpha \ll m_*, \\ m_*/\alpha, & \gamma < 1/2, m_* \ll \alpha. \end{cases} \quad (12)$$

Moreover, the k -critical threshold of the Bayes estimator satisfies

$$\alpha_k^{\text{Bayes}} = \Theta_k(k^{2\gamma} m_*^{(1-2\gamma)_+}), \quad (13)$$

where $x_+ := \max(0, x)$.

A proof of this result is discussed in Appendix A.

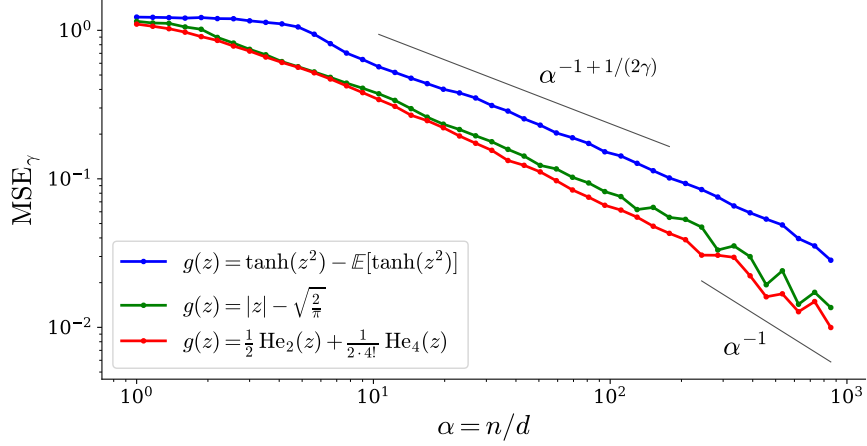


Figure 1: Weighted mean square error MSE_γ – see Def. 2.7 – of the spectral estimator of Def. 3.3 with preprocessing function $\mathcal{T}(y) = y/(1 + |y|)$, averaged over 70 instances. The target is given by the hierarchical multi-index model 2.1, with $g_k(z) = g(z) \forall k$, stated in the legend, and $a_k^* \propto k^{-\gamma}$, $\gamma = 1.3$. The covariates dimension is $d = 1000$, the feature space dimension is $m_\star = 10$.

3.2 Optimal Agnostic subspace recovery

While Theorem 3.2 provides a fundamental benchmark, an equally important question is whether the optimal reconstruction rates can be *efficiently* achieved by an algorithm which is agnostic of the underlying data distribution. In this section, we give an affirmative answer to this question by constructing an explicit spectral method achieving these rates.

Definition 3.3 (Spectral estimator). Given a *pre-processing* function $\mathcal{T} : \mathbb{R} \rightarrow \mathbb{R}$ on the labels, consider the symmetric random matrix

$$\mathbf{T} = \sum_{i=1}^n \mathcal{T}(y_i) \mathbf{x}_i \mathbf{x}_i^\top, \quad (14)$$

with spectrum $\lambda_1 \geq \lambda_2 \geq \dots \geq \lambda_d$. Define $r := \min\{i \in \mathbb{N} \mid \lambda_{i+1} - \lambda_{i+2} < C/\sqrt{d}\}$, for some arbitrary constant C . We define the spectral estimator

$$\hat{\mathbf{W}}^{\text{sp}} = (\hat{\mathbf{w}}_1, \dots, \hat{\mathbf{w}}_r)^\top \in \mathbb{R}^{r \times d} \quad (15)$$

where $\hat{\mathbf{w}}_k$ is the $k \in [r]$ eigenvector of \mathbf{T} corresponding to λ_k , normalized such that $\|\hat{\mathbf{w}}_k\|^2 = d$.

Such estimators have been studied in the context of multi-index models (Kovačević et al., 2025; Defilippis et al., 2025a) and proven to achieve the computationally optimal weak recovery threshold Troiani et al. (2025), for a tailored choice of the pre-processing function \mathcal{T} . Instead, here we consider \mathcal{T} to be data-agnostic, satisfying only the following mild conditions.

Assumption 3.4. Given $Y \sim \mathcal{N}(\sum_{k=1}^{m_\star} a_k^* g_k(z_k), \Delta)$ with $z \sim \mathcal{N}(\mathbf{0}, \mathbf{I}_{m_\star})$, we assume that:

- \mathcal{T} is bounded and there exists $\tau > 0$ such that

$$\tau = \inf\{c : \mathbb{P}(\mathcal{T}(Y) < c) = 1\}; \quad (16)$$

- $\mathbb{P}(\mathcal{T}(Y) = 0) < 1$.

Under Assumption 3.4, Kovačević et al. (2025) implies that, in the proportional high-dimensional limit $n, d \rightarrow \infty$ with $n = \Theta(d)$, the empirical spectrum of \mathbf{T} in eq. (14) converges to a bounded continuous density — refereed as the *bulk* — plus $r < m_\star$ isolated eigenvalues — refereed as the *spikes* — with r depending on the sample complexity $\alpha = n/d$.

The spikes are separated from the bulk by a finite gap and their corresponding eigenvectors exhibits a non-trivial correlation with $\text{span}(\mathbf{W}_\star)$. Therefore, the criterion described in Definition 3.3 (reminiscent of the heuristic “elbow” method in principal components analysis, see Fig. 3) for selecting the number of eigenvalues, agnostically retains only the informative components, discarding the noise contributions associated with the bulk. Note also that the choice of cutoff C/\sqrt{d} is arbitrary, as in general we want to separate the bulk with spacing $o_d(1)$ and the spikes with spacing $\Theta_d(1)$.

Remark 3.5 (GD interpretation of spectral method). Note that this spectral method also admits an interpretation in terms of a gradient descent algorithm. Indeed, considering a slightly modified loss than the pure square one, this matrix is nothing but the Hessian of the loss Bonnaire et al. (2025). The early dynamics of GD on the first layer of (10), for weights initialized on a sphere with small radius, will thus follow the proposed spectral method. This construction was recently used in Zhang et al. (2025) to show how two-layer neural networks identify features within the first few GD steps in the first layer weights. More precisely, they show that the early dynamics of a suitable gradient-based algorithm, reads as a power iteration

$$\mathbf{w}_k^{t+1} = \mathbf{w}_k^t - \nabla_{\mathbf{w}_k} \frac{1}{n} \sum_{i=1}^n \ell(y_i, \mathbf{a}^\top \sigma(\mathbf{W}^t \mathbf{x}_i)) \quad (17)$$

$$\approx (\mathbf{I}_d - a_k \sigma''(0) \mathbf{T}) \mathbf{w}_k^t, \quad (18)$$

where \mathbf{T} has the structure defined in eq. (14) with pre-processing $\mathcal{T} = \ell'(\cdot, 0)$, and ℓ' denoting the derivative of ℓ with respect to its second argument.

Our second main theoretical result shows that the data-agnostic spectral method defined above indeed achieves the optimal reconstruction rates of Theorem 3.2.

Theorem 3.6. *In the setting of Definitions 2.1, 2.2, under Assumption 2.3, denote $\hat{\mathbf{W}} = (\hat{\mathbf{W}}^{\text{sp}}, \mathbf{0}_{(m_\star - r) \times d}) \in \mathbb{R}^{m_\star \times d}$, where $\hat{\mathbf{W}}^{\text{sp}} \in \mathbb{R}^{r \times d}$, $r \leq m_\star$, is the spectral estimator defined in 3.3, with \mathcal{T} satisfying Assumption 3.4. Then, for $\alpha, m_\star \gg 1$,*

$$\text{MSE}_\gamma(\hat{\mathbf{W}}) = \Theta_{\alpha, m_\star}(\text{MMSE}_\gamma), \quad (19)$$

and the spectral estimator’s k -critical threshold α_k^{sp} satisfies

$$\alpha_k^{\text{sp}} = \Theta_k(\alpha_k^{\text{Bayes}}). \quad (20)$$

Remark 3.7. Note that, as the spectral method 3.3 retrieves $r \leq m_\star$ directions, we construct the full estimator by filling the remaining columns with zeros to evaluate MSE_γ in Def. 2.7. This zero-padding is harmless: the added zeros do not impact the derived scaling laws or the estimator’s agnostic nature.

In Appendix A.2, we show that the rates in Theorem 3.6 allow for an interpretation reminiscent of the “universal” error decomposition in Defilippi et al. (2025b). Let $k_\alpha \asymp \min(\alpha^{1/(2\gamma)}, m_\star)$ denote the number of weakly learnable features at sample complexity α – corresponding to the number of spikes of \mathbf{T} eq. (14). Then, the spectral mean-squared error decomposes into two main contributions: (i) the approximation error of the learnable concepts, scaling as $k_\alpha \cdot \Theta(\alpha^{-1})$; (ii) the underfitting due to the unlearnable concepts, scaling as $\Theta(\sum_{k=k_\alpha+1}^{m_\star} (a_k^*)^2)$.

Figure 1 shows the decay of the weighted MSE for three scale-free hierarchical model variants as a function of the sample complexity α , based on finite-size experiments, using the spectral method introduced in Definition 3.3. Notably, around $\alpha \asymp m_\star^{2\gamma} \approx 400$, we observe a crossover between the rates $\alpha^{-1+1/(2\gamma)}$ and m_\star/α , as predicted by Theorem 3.6. Figure 2 illustrates the sequential emergence of new concepts as sample complexity grows, visualized as spikes detaching from the eigenvalue bulk of the matrix \mathbf{T} in eq. (14).

3.3 Learning multi-index with neural networks

Finally, we turn our attention to the problem of learning hierarchical multi-index targets function with a two-layer neural network. In particular, we are interested in characterizing the scaling-laws associated with the excess risk in Equation (11) (rather than the reconstruction error in Equation (9)). Surprisingly, our main result in this section will show that the excess risk associated with a suitable training procedure described in Algorithm 1, achieves the optimal rates in Theorem 3.2.

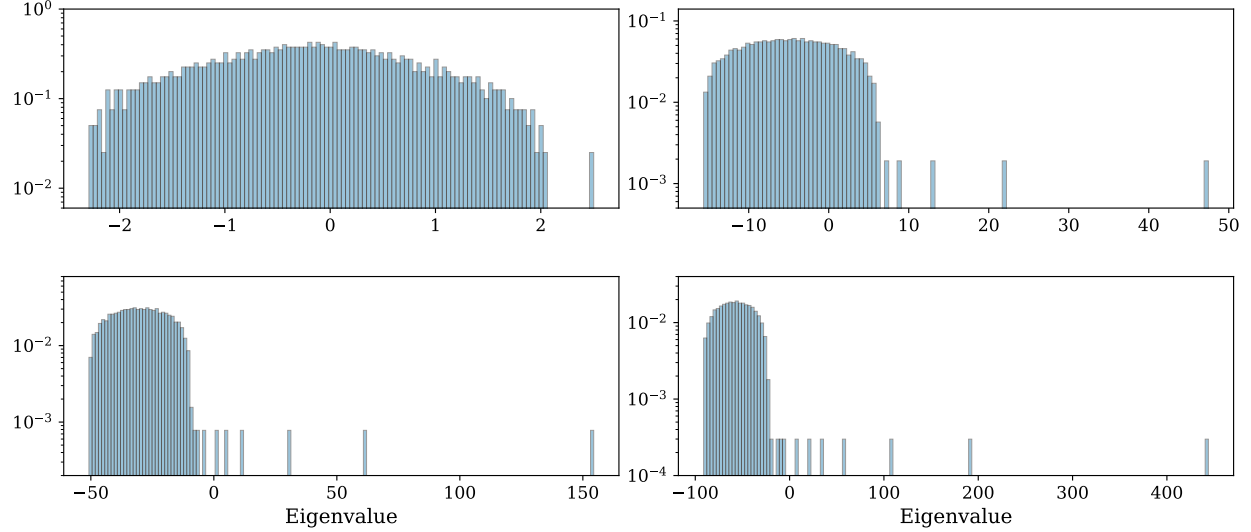


Figure 2: Empirical spectrum density of the matrix \mathbf{T} defined in eq. (14), with preprocessing function $\mathcal{T}(y) = y/(1 + |y|)$, at different sample complexities, highlighting the sequential emergence of concepts as the sample size increases. The target is given by a hierarchical multi-index model 2.1, with $g_k(z) = \frac{1}{2}\text{He}_2(z) + \frac{1}{24!}\text{He}_4(z) \forall k$ and $a_k \propto k^{-\gamma}$, $\gamma = 1.3$. The covariates dimension is $d = 1000$, the feature space dimension is $m_\star = 20$. **(top left)** $\alpha = 5$, **(top right)** $\alpha = 164$, **(bottom left)** $\alpha = 611$, **(bottom right)** $\alpha = 1638$.

Theorem 3.8. *In the setting of Definitions 2.1, 2.2, under Assumption 2.3, with $g_k^*, k \in [m_\star]$, polynomials of finite degree. There exist n_0 such that, for $n > n_0$, $p = \omega(n^{1/2})$, $\lambda = \Theta(n^{-1/2})$, the excess risk of eq. (11) for a two-layer neural network eq. (10), with σ bounded and continuous, trained according to Algorithm 1 satisfies*

$$R_{\text{NN}} = \Theta(\text{MMSE}_\gamma) + O(n^{-1/2}). \quad (21)$$

Remark 3.9. This final result demonstrate that neural networks can efficiently learn the target function, achieving the exact same rates as those of the optimal feature subspace recovery. We note that our results do not imply that these rates correspond to the decay of the Bayes risk, defined as $\mathbb{E}[(f_\star(\mathbf{x}) - \mathbb{E}[f_\star(\mathbf{x})|\mathbf{x}, \mathcal{D}])^2]$, and which constitutes a lower bound for the risk $R(\Theta)$ in Eq. (11). Nevertheless, we notice that under the hypothesis of a *fully specialized* Bayes-optimal estimator—i.e., assuming $d^{-1}\hat{\mathbf{W}}^{\text{Bayes}}(\mathbf{W}^*)^\top$ converges to a diagonal matrix in the high-dimensional limit—the risk for a network with matching architecture and Bayes weights, $f(\mathbf{x}) = \sum_{k=1}^{m_\star} a_k^* g_k(\hat{\mathbf{w}}_k^{\text{Bayes}})$, achieves the rates established in Theorem 3.2. We leave a more precise analysis of the optimal risk as a future direction.

4 Sketch of the proofs

We now discuss the key ideas involved in proving the results of Section 3.

Theorem 3.2 — The proof relies on establishing matching rates for the upper and lower bounds of MMSE_γ . In both case, we make sure of the decomposition of the target function into different directions, which we can recover sequentially. The upper bound is provided by the spectral method 3.3 in Theorem 3.6, which we discuss next.

The lower bound, derived in Appendix A.1, corresponds to the mean squared error of an oracle estimator granted access to the set of true weights $\{\mathbf{w}_h^*\}_{h \neq k}$ alongside the dataset. Conditioned on the remaining weights,

Algorithm 1 Spectral Initialization and Ridge Training

Input: Dataset $\mathcal{D} = (\mathbf{X}, \mathbf{y}) \in \mathbb{R}^{2n \times d} \times \mathbb{R}^{2n}$, hidden layer width m , regularization λ .
Output: Network parameters $\mathbf{W} \in \mathbb{R}^{p \times d}$, $\mathbf{a} \in \mathbb{R}^p$.

1. *Data Splitting*

Partition the dataset \mathcal{D} into two disjoint sets \mathcal{D}_1 and \mathcal{D}_2 such that $|\mathcal{D}_1| = |\mathcal{D}_2| = n$.

2. *Feature Learning (Spectral Initialization on \mathcal{D}_1)*

Compute the spectral estimator $\hat{\mathbf{W}}^{\text{sp}} \in \mathbb{R}^{r \times d}$ Def. 3.3 using \mathcal{D}_1 .

Sample a random matrix $\mathbf{Z} \in \mathbb{R}^{p \times r}$ with i.i.d. entries drawn from $\mathcal{N}(0, r^{-1})$.

Set first-layer weights: $\mathbf{W} = \mathbf{Z}\hat{\mathbf{W}}$.

3. *Readout Training (Ridge Regression on \mathcal{D}_2)*

Compute the feature matrix $\Psi \in \mathbb{R}^{n \times p}$ on \mathcal{D}_2 , where $\Psi_{ij} = \sigma(\langle \mathbf{w}_j, \mathbf{x}_i^{(2)} \rangle + b_j)$, $b_j \sim \mathcal{N}(0, 1)$.

Solve for the second-layer weights:

$$\mathbf{a} = (\Psi^\top \Psi + n\lambda \mathbf{I}_p)^{-1} \Psi^\top \mathbf{y}^{(2)}$$

return \mathbf{W}, \mathbf{a}

this formulation reduces to the Bayes-optimal estimator for the effective dataset $\mathcal{D}_k = \{(\mathbf{x}_i, a_k g_k(\langle \mathbf{x}_i, \mathbf{w}_k^* \rangle) + \sqrt{\Delta \xi_i})\}$, where ξ_i represents the same label noise as in the original problem and optimal MSE

$$\text{mmse}_k^{\text{oracle}} = \frac{1}{d^2} \mathbb{E}[\|\mathbb{E}[\mathbf{w}\mathbf{w}^\top | \mathcal{D}_k] - \mathbf{w}_k^* \mathbf{w}_k^{*\top}\|_F^2] \quad (22)$$

$$\leq \text{mmse}_k. \quad (23)$$

Consequently, the task can be analyzed as a single-index problem by leveraging the results in [Barbier et al. \(2019\)](#), which rigorously characterize the information-theoretic weak-recovery transition via the following free entropy functional:

$$\sup_{m \in [0, 1]} \{m + \log(1 - m) + 2\alpha \Psi_{\text{out}}(m)\}, \quad (24)$$

$$\Psi_{\text{out}}(m) :=$$

$$\mathbb{E}_{W, V, Y} \log \mathbb{E}_{w \sim \mathcal{N}(0, 1)} [\mathbb{P}(Y | \sqrt{m}V + \sqrt{1 - m}w)],$$

with $V, W \sim \mathcal{N}(0, 1)$ and $Y \sim \mathbb{P}(\cdot | \sqrt{m}V + \sqrt{1 - m}W)$.

In particular, this work establishes that information-theoretic weak recovery is achieved when the maximizer in eq. (24) satisfies $m \neq 0$, implying then $\text{mse}_k(\mathbf{w}_k^{\text{oracle}}) \rightarrow 1 - m^2$, in the high-dimensional limit. By expanding the potential $\Psi_{\text{out}}(m)$ around $a_k^* = 0$, we demonstrate that the oracle estimator weakly recovers \mathbf{w}_k^* when $\alpha = \Omega((a_k^*)^{-2})$, with error scaling as $\text{mse}_k(\mathbf{w}_k^{\text{oracle}}) \rightarrow \Theta_k((a_k^*)^2/\alpha)$, yielding the result.

Intuitively, this lower bound is tight because the effective signal-to-noise ratio for each index remains asymptotically equivalent to that of the original problem; specifically, the contribution of the other indices scales as $\Theta(1)$.

Theorem 3.6 – The proof (Appendix A.2) is based on an extension of the spectral methods analysis for multi-index models in [Defilippis et al. \(2025a\)](#); [Kovačević et al. \(2025\)](#). In particular, we show that, in the setting considered in the current manuscript, the eigenvectors of \mathbf{T} eq. (14) corresponding to the j largest eigenvalues, where r is the number of spikes detached from the spectral bulk (see Definition 3.3), correlate with $\mathbf{w}_1^*, \dots, \mathbf{w}_r^*$ individually. Furthermore, for large k , we show that the k -critical threshold and MSE_γ for the spectral estimator scale as the oracle estimator case considered in Appendix A.1.

Intuitively, this (constructive) upper bound matches the lower bound of the previous theorem because of the factorization of all indices. In multi-index models in full generality, the interaction between the direction can be arbitrary complicated, and the generic spectral methods more involved (See e.g. [Defilippis et al. \(2025a\)](#)). However, because of the hierarchical structure of the target, we can observe the direction one by one with a simpler spectral method sequentially without loosing too much information.

Theorem 3.8 – The argument (detailed in Appendix B) relies on a two-stage procedure: a spectral initialization followed by a random feature ridge regression (RFRR) on the retrieved subspace. First, leveraging the spectral analysis of the matrix \mathbf{T} defined in eq. (14), we model the true weights \mathbf{w}_i^* as a perturbation of the spectral estimator’s retrieved directions $\hat{\mathbf{w}}_i$ (for $i \leq r$). Next, we define the projected input $\mathbf{s} = (\hat{\mathbf{w}}_1, \dots, \hat{\mathbf{w}}_r)^\top \mathbf{x}$. By Taylor-expanding the activation functions around these retrieved directions, the target decomposes into a ‘clean’ signal component and an effective noise term:

$$y \approx \sum_{k=1}^r a_k^* g_k(s_k) + \sqrt{\Delta_{\text{eff}}} \xi, \quad (25)$$

where ξ acts as a centered, unit-variance noise. Crucially, the effective variance Δ_{eff} captures three distinct error sources: (i) the intrinsic label noise Δ ; (ii) the contribution from the unlearned indices ($i > r$); and (iii) the error arising from the spectral approximation. Finally, we analyze the performance of RFRR trained on the projected inputs \mathbf{s} . Invoking standard results on random feature regression [Rudi and Rosasco \(2017\)](#), we show that with sufficient over-parameterization ($m \asymp \sqrt{n}$), the RFRR estimation error decays as $O(n^{-1/2})$. Since this decay is faster than the rates governing both the spectral reconstruction and the unlearned signal components, the RFRR error is subleading. Consequently, the asymptotic excess risk is dominated solely by the excess effective noise $\Delta_{\text{eff}} - \Delta$, yielding the matching rates.

5 Conclusions, discussions, and limitations

Our results suggest a unifying picture for representation learning and scaling laws in shallow neural networks.

First, we show that the scaling exponents previously observed for quadratic networks by [Defilippis et al. \(2025b\)](#) are in fact *universal*. Remarkably, the same rates coincide with classical minimax bounds for LASSO and matrix compressed sensing under quasi-sparse assumptions. This indicates that quadratic and diagonal models already capture the essential statistical structure governing feature learning in a much broader class of neural architectures. On a technical level, an importance difference is that the quadratic neural network analysis hold in the regime where $m_* = O(d)$, while where m_* is taken to be large but small compared to n, d . Our results showing that these rates coincide suggest that the analysis can be extended beyond this limit, and closing this gap is an interesting open question for future work.

Second, our analysis reproduces several empirical phenomena observed in trained networks. After spectral (or Hessian-based) training, the learned weight matrices exhibit structured, non-random spectra closely resembling those reported in empirical studies of attention layers and deep networks. In particular, the resulting singular-value distributions display a non-trivial bulk and heavy-tailed behavior, consistent with observations across architectures and scales [Mahoney and Martin \(2019\)](#); [Martin et al. \(2021\)](#); [Thamm et al. \(2024\)](#). Our theory provides a first-principles explanation of how such spectral structure emerges from data and target geometry, and clarifies its role in generalization.

More broadly, we provide a solvable setting in which two key empirical phenomena—neural scaling laws and progressive feature emergence—arise simultaneously. As the sample size increases, learning proceeds through a sequence of sharp transitions, with new directions in representation space becoming detectable one after another. This produces plateaus and abrupt drops in error, mirroring observations in real neural networks [Wei et al. \(2022\)](#); [Arora and Goyal \(2023\)](#); [Kunin et al. \(2025\)](#); [Schaeffer et al. \(2023\)](#); [Ren et al. \(2025\)](#). Our results show that both scaling laws and emergence can be understood within a single, tractable theoretical framework.

An important open direction is to understand to what extent these optimal rates can be achieved by stochastic gradient descent. While recent works have analyzed SGD dynamics in related settings [Ren et al. \(2025\)](#); [Ben Arous et al. \(2025\)](#), it remains an open question whether SGD can provably attain the

Bayes-optimal scaling laws identified here without spectral initialization or explicit regularization. Addressing this question would further bridge the gap between optimal statistical theory and practical training dynamics. For quadratic problems, [Defilippis et al. \(2024\)](#) showed that full batch gradient descent can attain those rates with proper regularization.

Finally, we note that our analysis deliberately relies on simplifying assumptions—most notably isotropic Gaussian data, two-layer architectures, and an asymptotic high-dimensional limit—which are essential to obtain sharp, non-perturbative results and exact scaling predictions. In this sense, the assumptions underlying multi-index models are both a limitation and a strength: they isolate the minimal mechanisms governing representation learning while remaining analytically tractable. Despite these simplifications, the resulting theory reproduces a wide range of empirical phenomena observed in trained attention models, including progressive feature emergence, structured weight spectra, and optimal scaling behavior. We view this work as establishing a principled rigorous foundation on which more realistic data distributions, architectures, and training dynamics can be systematically incorporated in future work.

Acknowledgements

We would like to thank Yatin Dandi, Vittorio Erba and Lenka Zdeborova for insightful discussions. BL and LD were supported by the French government, managed by the National Research Agency (ANR), under the France 2030 program with the reference “ANR-23-IACL-0008” and the Choose France - CNRS AI Rising Talents program. FK acknowledge funding from the Swiss National Science Foundation grants OperaGOST (grant number 200021 200390) and DSGIANGO (grant number 225837). This work was supported by the Simons Collaboration on the Physics of Learning and Neural Computation via the Simons Foundation grant (#1257412).

References

- E. Abbe, E. B. Adserà, and T. Misiakiewicz. Sgd learning on neural networks: leap complexity and saddle-to-saddle dynamics. In G. Neu and L. Rosasco, editors, *Proceedings of Thirty Sixth Conference on Learning Theory*, volume 195 of *Proceedings of Machine Learning Research*, pages 2552–2623. PMLR, 12–15 Jul 2023. URL <https://proceedings.mlr.press/v195/abbe23a.html>.
- M. Andriushchenko, A. V. Varre, L. Pillaud-Vivien, and N. Flammarion. Sgd with large step sizes learns sparse features. In *International Conference on Machine Learning*, pages 903–925. PMLR, 2023.
- S. Arora and A. Goyal. A theory for emergence of complex skills in language models. *arXiv preprint arXiv:2307.15936*, 2023.
- A. Atanasov, J. A. Zavatone-Veth, and C. Pehlevan. Scaling and renormalization in high-dimensional regression. *arXiv preprint arXiv:2405.00592*, 2024.
- B. Aubin, A. Maillard, F. Krzakala, N. Macris, L. Zdeborová, et al. The committee machine: Computational to statistical gaps in learning a two-layers neural network. *Advances in Neural Information Processing Systems*, 31, 2018.
- D. Babichev and F. Bach. Slice inverse regression with score functions. *Electronic Journal of Statistics*, 12(1): 1507 – 1543, 2018. doi: 10.1214/18-EJS1428. URL <https://doi.org/10.1214/18-EJS1428>.
- Y. Bahri, E. Dyer, J. Kaplan, J. Lee, and U. Sharma. Explaining neural scaling laws. *Proceedings of the National Academy of Sciences*, 121(27):e2311878121, 2024.
- J. Barbier, F. Krzakala, N. Macris, L. Miolane, and L. Zdeborová. Phase transitions, optimal errors and optimality of message-passing in generalized linear models. *CoRR*, abs/1708.03395, 2017. URL <http://arxiv.org/abs/1708.03395>.

J. Barbier, F. Krzakala, N. Macris, L. Miolane, and L. Zdeborová. Optimal errors and phase transitions in high-dimensional generalized linear models. *Proceedings of the National Academy of Sciences*, 116(12):5451–5460, 2019. doi: 10.1073/pnas.1802705116. URL <https://www.pnas.org/doi/abs/10.1073/pnas.1802705116>.

M. Bayati and A. Montanari. The dynamics of message passing on dense graphs, with applications to compressed sensing. *IEEE Transactions on Information Theory*, 57(2):764–785, 2011.

G. Ben Arous, M. A. Erdogdu, N. M. Vural, and D. Wu. Learning quadratic neural networks in high dimensions: SGD dynamics and scaling laws. *arXiv preprint arXiv:2508.03688*, 2025.

R. Berthier, A. Montanari, and P.-M. Nguyen. State evolution for approximate message passing with non-separable functions. *Information and Inference: A Journal of the IMA*, 9(1):33–79, 2020.

T. Bonnaire, G. Biroli, and C. Cammarota. The role of the time-dependent hessian in high-dimensional optimization. *Journal of Statistical Mechanics: Theory and Experiment*, 2025(8):083401, 2025.

B. Bordelon, A. Canatar, and C. Pehlevan. Spectrum dependent learning curves in kernel regression and wide neural networks. In *International Conference on Machine Learning*, pages 1024–1034. PMLR, 2020.

B. Bordelon, A. Atanasov, and C. Pehlevan. A dynamical model of neural scaling laws. *Proceedings of the 41st International Conference on Machine Learning*, 2024. arXiv preprint arXiv:2402.01092.

B. Bordelon, A. Atanasov, and C. Pehlevan. How feature learning can improve neural scaling laws. *Journal of Statistical Mechanics: Theory and Experiment*, 2025(8):084002, 2025.

G. Braun, B. Loureiro, H. Q. Minh, and M. Imaizumi. Fast escape, slow convergence: Learning dynamics of phase retrieval under power-law data. *arXiv preprint arXiv:2511.18661*, 2025.

T. Brown, B. Mann, N. Ryder, M. Subbiah, J. D. Kaplan, P. Dhariwal, A. Neelakantan, P. Shyam, G. Sastry, A. Askell, et al. Language models are few-shot learners. *Advances in neural information processing systems*, 33:1877–1901, 2020.

A. Caponnetto and E. De Vito. Optimal rates for the regularized least-squares algorithm. *Foundations of Computational Mathematics*, 7(3):331–368, 2007.

A. Christmann and I. Steinwart. Support vector machines. *Systems and Virtualization Management. Standards and New Technologies*, 2008.

H. Cui, B. Loureiro, F. Krzakala, and L. Zdeborová. Generalization error rates in kernel regression: The crossover from the noiseless to noisy regime. *Advances in Neural Information Processing Systems*, 34: 10131–10143, 2021.

H. Cui, B. Loureiro, F. Krzakala, and L. Zdeborová. Error scaling laws for kernel classification under source and capacity conditions. *Machine Learning: Science and Technology*, 4(3):035033, 2023.

A. Damian, J. Lee, and M. Soltanolkotabi. Neural networks can learn representations with gradient descent. In *Conference on Learning Theory*, pages 5413–5452. PMLR, 2022.

A. Damian, L. Pillaud-Vivien, J. D. Lee, and J. Bruna. Computational-statistical gaps in gaussian single-index models. *arXiv preprint arXiv:2403.05529*, 2024.

Y. Dandi, F. Krzakala, B. Loureiro, L. Pesce, and L. Stephan. How two-layer neural networks learn, one (giant) step at a time. *Journal of Machine Learning Research*, 25(349):1–65, 2024.

L. Defilippis, B. Loureiro, and T. Misiakiewicz. Dimension-free deterministic equivalents and scaling laws for random feature regression. *Advances in Neural Information Processing Systems*, 37:104630–104693, 2024.

L. Defilippis, Y. Dandi, P. Mergny, F. Krzakala, and B. Loureiro. Optimal spectral transitions in high-dimensional multi-index models, 2025a. URL <https://arxiv.org/abs/2502.02545>.

L. Deflippis, Y. Xu, J. Girardin, E. Troiani, V. Erba, L. Zdeborová, B. Loureiro, and F. Krzakala. Scaling laws and spectra of shallow neural networks in the feature learning regime. *arXiv preprint arXiv:2509.24882*, 2025b.

D. L. Donoho. Compressed sensing. *IEEE Transactions on information theory*, 52(4):1289–1306, 2006.

D. L. Donoho, M. Gavish, and A. Montanari. The phase transition of matrix recovery from Gaussian measurements matches the minimax mse of matrix denoising. *Proceedings of the National Academy of Sciences*, 110(21):8405–8410, 2013.

R. Dudeja, Y. M. Lu, and S. Sen. Universality of approximate message passing with semirandom matrices. *The Annals of Probability*, 51(5):1616–1683, 2023.

V. Erba, E. Troiani, L. Zdeborová, and F. Krzakala. The nuclear route: Sharp asymptotics of ERM in overparameterized quadratic networks. *NeurIPS 2025*, 2025. arXiv preprint arXiv:2505.17958.

O. Y. Feng, R. Venkataraman, C. Rush, and R. J. Samworth. A unifying tutorial on approximate message passing. *Foundations and Trends® in Machine Learning*, 15(4):335–536, 2022. ISSN 1935-8237. doi: 10.1561/2200000092. URL <http://dx.doi.org/10.1561/2200000092>.

C. Gerbelot and R. Berthier. Graph-based approximate message passing iterations. *Information and Inference: A Journal of the IMA*, 12(4):2562–2628, 2023.

S. Gunasekar, B. E. Woodworth, S. Bhojanapalli, B. Neyshabur, and N. Srebro. Implicit regularization in matrix factorization. *Advances in neural information processing systems*, 30, 2017.

J. Hoffmann, S. Borgeaud, A. Mensch, E. Buchatskaya, T. Cai, E. Rutherford, D. de Las Casas, L. A. Hendricks, J. Welbl, A. Clark, et al. An empirical analysis of compute-optimal large language model training. *Advances in neural information processing systems*, 35:30016–30030, 2022.

A. Javanmard and A. Montanari. State evolution for general approximate message passing algorithms, with applications to spatial coupling. *Information and Inference: A Journal of the IMA*, 2(2):115–144, 2013.

J. Kaplan, S. McCandlish, T. Henighan, T. B. Brown, B. Chess, R. Child, S. Gray, A. Radford, J. Wu, and D. Amodei. Scaling laws for neural language models. *arXiv preprint arXiv:2001.08361*, 2020.

F. Kovačević, Y. Zhang, and M. Mondelli. Spectral estimators for multi-index models: Precise asymptotics and optimal weak recovery. *arXiv preprint arXiv:2502.01583*, 2025.

F. Kovačević, Z. Yihan, and M. Mondelli. Spectral estimators for multi-index models: Precise asymptotics and optimal weak recovery. In N. Haghtalab and A. Moitra, editors, *Proceedings of Thirty Eighth Conference on Learning Theory*, volume 291 of *Proceedings of Machine Learning Research*, pages 3354–3404. PMLR, 30 Jun–04 Jul 2025. URL <https://proceedings.mlr.press/v291/kovacevic25a.html>.

D. Kunin, G. L. Marchetti, F. Chen, D. Karkada, J. B. Simon, M. R. DeWeese, S. Ganguli, and N. Miolane. Alternating gradient flows: A theory of feature learning in two-layer neural networks. *arXiv preprint arXiv:2506.06489*, 2025.

F. Kunstner and F. Bach. Scaling laws for gradient descent and sign descent for linear bigram models under Zipf’s law. *arXiv preprint arXiv:2505.19227*, 2025.

K.-C. Li. Sliced inverse regression for dimension reduction. *Journal of the American Statistical Association*, 86(414):316–327, 1991.

Y. M. Lu and G. Li. Phase transitions of spectral initialization for high-dimensional non-convex estimation. *Information and Inference: A Journal of the IMA*, 9(3):507–541, 2020.

M. Mahoney and C. Martin. Traditional and heavy tailed self regularization in neural network models. In *International Conference on Machine Learning*, pages 4284–4293. PMLR, 2019.

A. Maillard, F. Krzakala, Y. M. Lu, and L. Zdeborová. Construction of optimal spectral methods in phase retrieval. In *Mathematical and Scientific Machine Learning*, pages 693–720. PMLR, 2022.

A. Maillard, E. Troiani, S. Martin, F. Krzakala, and L. Zdeborová. Bayes-optimal learning of an extensive-width neural network from quadratically many samples. *Advances in Neural Information Processing Systems*, 37:82085–82132, 2024.

S. Mallat. *A wavelet tour of signal processing*. Elsevier, 1999.

A. Maloney, D. A. Roberts, and J. Sully. A solvable model of neural scaling laws. *arXiv preprint arXiv:2210.16859*, 2022.

C. H. Martin and M. W. Mahoney. Implicit self-regularization in deep neural networks: Evidence from random matrix theory and implications for learning. *Journal of Machine Learning Research*, 22(165):1–73, 2021.

C. H. Martin, T. Peng, and M. W. Mahoney. Predicting trends in the quality of state-of-the-art neural networks without access to training or testing data. *Nature Communications*, 12(1):4122, 2021.

S. Martin, G. Biroli, and F. Bach. High-dimensional analysis of gradient flow for extensive-width quadratic neural networks. *arXiv preprint arXiv:2601.10483*, 2026.

M. Mondelli and A. Montanari. Fundamental limits of weak recovery with applications to phase retrieval. *Foundations of Computational Mathematics*, 19(3):703–773, Jun 2019. ISSN 1615-3383. doi: 10.1007/s10208-018-9395-y. URL <https://doi.org/10.1007/s10208-018-9395-y>.

R. O’Donnell. *Analysis of Boolean Functions*. Cambridge University Press, 2014.

E. Paquette, C. Paquette, L. Xiao, and J. Pennington. 4+3 phases of compute-optimal neural scaling laws. *Advances in Neural Information Processing Systems*, 37:16459–16537, 2024.

A. Rahimi and B. Recht. Random features for large-scale kernel machines. In J. Platt, D. Koller, Y. Singer, and S. Roweis, editors, *Advances in Neural Information Processing Systems*, volume 20. Curran Associates, Inc., 2007. URL https://proceedings.neurips.cc/paper_files/paper/2007/file/013a006f03dbc5392effeb8f18fda755-Paper.pdf.

G. Raskutti, M. J. Wainwright, and B. Yu. Minimax rates of estimation for high-dimensional linear regression over ℓ_q -balls. *IEEE transactions on information theory*, 57(10):6976–6994, 2011.

Y. Ren, E. Nichani, D. Wu, and J. D. Lee. Emergence and scaling laws in SGD learning of shallow neural networks. *arXiv preprint arXiv:2504.19983*, 2025.

A. Rudi and L. Rosasco. Generalization properties of learning with random features. In I. Guyon, U. V. Luxburg, S. Bengio, H. Wallach, R. Fergus, S. Vishwanathan, and R. Garnett, editors, *Advances in Neural Information Processing Systems*, volume 30. Curran Associates, Inc., 2017. URL https://proceedings.neurips.cc/paper_files/paper/2017/file/61b1fb3f59e28c67f3925f3c79be81a1-Paper.pdf.

A. Saxe, J. McClelland, and S. Ganguli. Exact solutions to the nonlinear dynamics of learning in deep linear neural networks. In *Proceedings of the International Conference on Learning Representations 2014*. International Conference on Learning Representations 2014, 2014.

R. Schaeffer, B. Miranda, and S. Koyejo. Are emergent abilities of large language models a mirage? *Advances in neural information processing systems*, 36:55565–55581, 2023.

D. Soudry, E. Hoffer, M. S. Nacson, S. Gunasekar, and N. Srebro. The implicit bias of gradient descent on separable data. *Journal of Machine Learning Research*, 19(70):1–57, 2018.

S. Spigler, M. Geiger, and M. Wyart. Asymptotic learning curves of kernel methods: empirical data versus teacher–student paradigm. *Journal of Statistical Mechanics: Theory and Experiment*, 2020(12):124001, 2020.

M. Thamm, M. Staats, and B. Rosenow. Random matrix theory analysis of neural network weight matrices. In *High-dimensional Learning Dynamics 2024: The Emergence of Structure and Reasoning*, 2024.

E. Troiani, Y. Dandi, L. Defilippis, L. Zdeborova, B. Loureiro, and F. Krzakala. Fundamental computational limits of weak learnability in high-dimensional multi-index models. In Y. Li, S. Mandt, S. Agrawal, and E. Khan, editors, *Proceedings of The 28th International Conference on Artificial Intelligence and Statistics*, volume 258 of *Proceedings of Machine Learning Research*, pages 2467–2475. PMLR, 03–05 May 2025. URL <https://proceedings.mlr.press/v258/troiani25a.html>.

Z. Wang, A. Engel, A. D. Sarwate, I. Dumitriu, and T. Chiang. Spectral evolution and invariance in linear-width neural networks. *Advances in neural information processing systems*, 36:20695–20728, 2023.

J. Wei, Y. Tay, R. Bommasani, C. Raffel, B. Zoph, S. Borgeaud, D. Yogatama, M. Bosma, D. Zhou, D. Metzler, et al. Emergent abilities of large language models. *arXiv preprint arXiv:2206.07682*, 2022.

R. Worschech and B. Rosenow. Analyzing neural scaling laws in two-layer networks with power-law data spectra. *arXiv preprint arXiv:2410.09005*, 2024.

A. Wortsman and B. Loureiro. Kernel ridge regression under power-law data: spectrum and generalization. *arXiv preprint arXiv:2510.04780*, 2025.

Y. Xu, A. Maillard, L. Zdeborová, and F. Krzakala. Fundamental limits of matrix sensing: Exact asymptotics, universality, and applications. *COLT 2025*, 2025. arXiv preprint arXiv:2503.14121.

M. Yuan. On the identifiability of additive index models. *Statistica Sinica*, pages 1901–1911, 2011.

B. Zhang, Z. Wang, H. Fu, and J. D. Lee. Neural networks learn generic multi-index models near information-theoretic limit, 2025. URL <https://arxiv.org/abs/2511.15120>.

Q. Zou and H. Yang. A concise tutorial on approximate message passing. *arXiv preprint arXiv:2201.07487*, 2022.

A Proof of Theorems 3.2 and 3.6

In this section, we prove the information-theoretic results stated in Theorem 3.2. In particular, we derive matching bounds for the MMSE_γ , defined 3.1, and the k -critical threshold α_k (Definition 2.6). In Appendix A.1, we analyze an oracle estimator that exploits additional information to achieve a weighted mean-squared error smaller than MMSE_γ . Finally, in Appendix A.2, we complete the proof by characterizing the scaling laws and k -critical thresholds of the spectral estimator defined in 3.3, which simultaneously establishes the results in Theorem 3.6.

A.1 Lower bound

Definition A.1 (Oracle Estimator). Consider a dataset $\mathcal{D} = \{(\mathbf{x}_i, y_i) \in \mathbb{R}^d \times \mathbb{R}\}_{i \in [n]}$, where the labels are generated by a multi-index model $y \sim \mathbb{P}(\cdot | \langle \mathbf{w}_1^*, \mathbf{x} \rangle, \dots, \langle \mathbf{w}_{m_*}^*, \mathbf{x} \rangle)$, with weights \mathbf{W}^* drawn from a distribution $\mathbb{P}_{\mathbf{W}}$. We define the Oracle Estimator as the matrix $\mathbf{W}^{\text{oracle}} \in \mathbb{R}^{m \times d}$ with rows

$$\mathbf{w}_k^{\text{oracle}} = \arg \min_{\mathbf{w}} \mathbb{E} [\|\mathbf{w}_k \mathbf{w}_k^\top - \mathbf{w}_k^* \mathbf{w}_k^{*\top}\|_F^2 | \mathcal{D}, \{\mathbf{w}_h\}_{h \neq k}], k \in [m_*]. \quad (26)$$

Analogously to the Bayes-optimal estimator case, the weighed mean-squared error $\text{MSE}_\gamma(\mathbf{W}^{\text{oracle}})$ is lower bounded by

$$\text{MMSE}_\gamma^{\text{oracle}} = \frac{1}{d^2} \sum_{k=1}^{m_*} (a_k^*)^2 \mathbb{E} [\|\mathbb{E}[\mathbf{w}_k \mathbf{w}_k^\top | \mathcal{D}, \{\mathbf{w}_h^*\}_{h \neq k}] - \mathbf{w}_k^* \mathbf{w}_k^{*\top}\|_F^2]. \quad (27)$$

As a consequence of the law of total variance

$$d^2 \text{mmse}_k := \mathbb{E} [\text{Cov}(\mathbf{w}_k \mathbf{w}_k^\top | \mathcal{D})] \quad (28)$$

$$= \mathbb{E} [\text{Cov}(\mathbf{w}_k \mathbf{w}_k^\top | \mathcal{D}, \{\mathbf{w}_h\}_{h \neq k})] + \underbrace{\mathbb{E} [\text{Cov}_{\{\mathbf{w}_h\}_{h \neq k}} (\mathbb{E} [\mathbf{w}_k \mathbf{w}_k^\top | \mathcal{D}, \{\mathbf{w}_h\}_{h \neq k}])]}_{\geq 0} \quad (29)$$

$$\geq d^2 \mathbb{E} [\|\mathbb{E}[\mathbf{w}_k \mathbf{w}_k^\top | \mathcal{D}, \{\mathbf{w}_h^*\}_{h \neq k}] - \mathbf{w}_k^* \mathbf{w}_k^{*\top}\|_F^2]. \quad (30)$$

Therefore,

$$\text{MMSE}_\gamma^{\text{oracle}} \leq \text{MMSE}_\gamma. \quad (31)$$

We now focus on the specific setting of our interest defined in Section 2. For each index $k \in [m_*]$, conditioning on $\{\mathbf{w}_h\}_{h \neq k}$, the problem of the optimal estimation of \mathbf{w}_k^* becomes statistically equivalent to the Bayes-optimal estimation given a dataset $\mathcal{D}_k := \{(\mathbf{x}_\nu, \bar{y}_\nu)\}_{\nu \in [n]}$, where the labels are generated by the single-index model

$$\bar{y}_i = a_k^* g_k(\langle \mathbf{w}_k^*, \mathbf{x}_i \rangle) + \sqrt{\Delta} \xi_i, \quad (32)$$

where ξ_i is the same label noise as in the original dataset. We can now characterize the oracle estimator using the results from the literature on *single-index models*, in particular [Barbier et al. \(2019\)](#). In Appendix C we show that the information-theoretic weak recovery threshold for single-index models is a monotonic decreasing function of the signal-to-noise ratio. Combined with Assumption 2.3, this implies that the sequence of k -critical thresholds α_k is bounded by strictly increasing functions.² In particular, the first result in Corollary C.4 implies that the sequence is bounded by

$$\alpha_k^{\text{oracle}} = \Theta((a_k^*)^{-2}) = \Theta(k^{2\gamma} m_*^{(1-2\gamma)+}), \quad (33)$$

with $(x)_+ = \max(0, x)$. Further, denoting by k_α the largest index k such that $\alpha > \alpha_k$, i.e. $k_\alpha = \max(m_*, \Theta(\alpha^{1/(2\gamma)}))$ for $\gamma > 1/2$ or $k_\alpha = \max(m_*, \Theta(m_*^{-1+1/(2\gamma)} \alpha^{1/(2\gamma)}))$ for $\gamma < 1/2$, and exploiting

²If $g_k = g$, $\forall k$, the sequence α_k^{oracle} itself is strictly increasing.

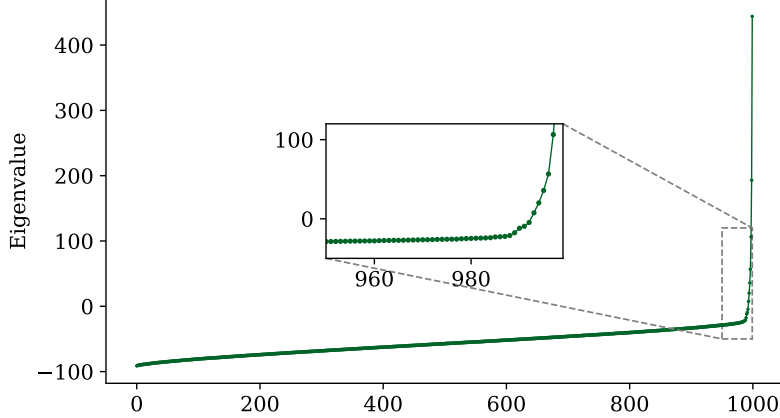


Figure 3: Empirical spectrum of \mathbf{T} eq. (14) with preprocessing $\mathcal{T}(y) = y/(1 + |y|)$, for a hierarchical multi-index model with $g_k(z) = \frac{1}{2}\text{He}_2(z) + \frac{1}{2 \cdot 4!}\text{He}_4(z)$ and $\gamma = 1.3$. The covariates dimension is $d = 1000$, while the feature space dimension is $m_* = 20$. The figure illustrates the change in scale of the eigenvalue gaps, transitioning from the informative spikes ($\Theta_d(1)$) to the uninformative bulk ($o_d(1)$). This behavior forms the basis of the selection method described in Def. 3.3.

the second result in Corollary C.4,

$$\text{MMSE}_\gamma^{\text{oracle}} = \left(\sum_{k=1}^{k_\alpha} + \sum_{k=k_\alpha+1}^{m_*} \right) (a_k^*)^2 \mathbb{E} [\|\mathbb{E}[\mathbf{w}_k \mathbf{w}_k^\top | \mathcal{D}, \{\mathbf{w}_h^*\}_{h \neq k}] - \mathbf{w}_k^* \mathbf{w}_k^{*\top}\|_F^2] \quad (34)$$

$$\geq C \left(\sum_{k=1}^{k_\alpha} \frac{(a_k^*)^2}{(a_k^*)^2 \alpha} + \sum_{k=k_\alpha+1}^{m_*} (a_k^*)^2 \right) \quad (35)$$

$$= \begin{cases} \Theta(\alpha^{-1+1/(2\gamma)}), & \gamma > 1/2, \alpha \ll m_*^{2\gamma} \\ \Theta(m_*/\alpha), & \gamma > 1/2, \alpha \gg m_*^{2\gamma} \\ \Theta(1), & \gamma < 1/2, \alpha \ll m_* \\ \Theta(m_*/\alpha), & \gamma < 1/2, \alpha \gg m_* \end{cases} \quad (36)$$

Note that we have used

$$\sum_{k=k_\alpha+1}^{m_*} k^{-2\gamma} = \begin{cases} \Theta(k_\alpha^{1-2\gamma}), & \gamma > 1/2, \\ \Theta(m_*^{1-2\gamma}), & \gamma < 1/2. \end{cases} \quad (37)$$

In eq. (35), the first term is a lower bound to the (weighted) mean-squared error of weakly recovered features, while the second corresponds to the underfitting contribution of the unlearned ones.

A.2 Upper bound – (Theorem 3.6)

By definition, any estimator that is a function of the dataset only has a weighted mean-squared error larger than MMSE_γ . In this section we consider the spectral method defined in 3.3. The following Theorem, proven in Kovačević et al. (2025), is valid for generic Gaussian multi-index models with m_* indices. We refer to the original work for further details. In the rest of the section we denote by \mathbb{E} the expected value with respect to $\mathbf{z} \sim \mathcal{N}(\mathbf{0}_{m_*}, \mathbf{I}_{m_*})$ and $Y \sim \mathcal{N}(\sum_{k=1}^{m_*} (a_k^*)^2 g_k(z_k), \Delta)$.

Theorem A.2 (Theorem 4.1 in Kovačević et al. (2025)). *Let $\mathcal{T} : \mathbb{R} \rightarrow \mathbb{R}$ be a preprocessing function subject to Assumption 3.4 and \mathbf{T} defined as in eq. 14. Let $t_1 \geq t_2 \geq \dots \geq t_r \geq \tau$, for some $r \in [m]$, be all the solutions to*

$$\det \left(\alpha \mathbb{E} \left[\frac{(\mathbf{z} \mathbf{z}^\top - \mathbf{I}_m) \mathcal{T}(Y)}{t - \mathcal{T}(Y)} \right] - \mathbf{I}_p \right) = 0 \quad (38)$$

such that

$$t_k \geq \bar{t}_\alpha := \arg \min_{t \geq \tau} \zeta_\alpha(t), \quad \forall k \in [j], \quad (39)$$

where

$$\zeta_\alpha(t) := t \left(1 + \alpha \mathbb{E} \left[\frac{\mathcal{T}(Y)}{t - \mathcal{T}(Y)} \right] \right). \quad (40)$$

Then, denote $\lambda_1^T, \dots, \lambda_{m_*}^T$ the largest m_* eigenvalues of \mathbf{T} . For the top r eigenvalues it holds that

$$\lambda_1^T, \dots, \lambda_r^T \xrightarrow{\text{a.s.}} \zeta_\alpha(t_1), \dots, \zeta_\alpha(t_r), \quad (41)$$

and for the remaining $m_* - r$ eigenvectors it holds that

$$\lambda_{r+1}^T, \dots, \lambda_{m_*}^T \xrightarrow{\text{a.s.}} \zeta_\alpha(\bar{t}_\alpha). \quad (42)$$

As a first result, we derive a bound for α_k .

Consider the matrix in eq. (38)

$$\mathbb{E} \left[\frac{(\mathbf{z}\mathbf{z}^\top - \mathbf{I}_m)\mathcal{T}(Y)}{t - \mathcal{T}(Y)} \right] = \mathbb{E}_Y \left[\mathbf{G}(Y) \frac{\mathcal{T}(Y)}{t - \mathcal{T}(Y)} \right], \quad (43)$$

with $\mathbf{G}(y) = \mathbb{E}[\mathbf{z}\mathbf{z}^\top - \mathbf{I}_m | Y = y]$. It is straightforward to show that it is a diagonal matrix, due to the parity of each function g_k . Indeed, given $k \neq h$,

$$G_{kh}(y) = \mathbb{E}[z_k z_h | y] \propto \int e^{-\|\mathbf{z}\|^2/2} \exp \left(- \left(y - \sum_{k=1}^m a_k g_k(z_k) \right)^2 / (2\Delta) \right) z_h z_k d\mathbf{z} = 0. \quad (44)$$

For simplicity, we denote $G_k(y) := G_{kk}(y)$. Therefore, the solutions of eq. (38) coincides with the solutions of

$$\alpha^{-1} = \mathbb{E} \left[\frac{\mathcal{T}(y)}{t - \mathcal{T}(Y)} G_k(Y) \right], \quad k \in [m]. \quad (45)$$

Further, note that, by definition \bar{t}_α is the solution of

$$\alpha^{-1} = \mathbb{E} \left[\left(\frac{\mathcal{T}(Y)}{t - \mathcal{T}(Y)} \right)^2 \right]. \quad (46)$$

A spectral transition occurs if, for sample complexity α and index $k \in [m]$, the value \bar{t}_α is also solution of eq. (45). Indeed by Theorem 4.2 in [Kovačević et al. \(2025\)](#) – which characterizes the overlap of the principal r eigenvalues, such sample complexity corresponds to the k -critical threshold α_k . This implies, for $\alpha = \alpha_k^{\text{sp}}$

$$\begin{cases} (\alpha_k^{\text{sp}})^{-1} = \mathbb{E}_y \left[\frac{\mathcal{T}(Y)}{t - \mathcal{T}(Y)} G_k(Y) \right] \\ (\alpha_k^{\text{sp}})^{-1} = \mathbb{E}_y \left[\left(\frac{\mathcal{T}(Y)}{t - \mathcal{T}(Y)} \right)^2 \right]. \end{cases} \quad (47)$$

In order to characterize the threshold, we consider the following expansions for small SNR $a_k^* \ll 1$. Define Z the marginal distribution of Y

$$Z(y) := \frac{1}{\sqrt{2\pi\Delta}} \mathbb{E}_\mathbf{z} \left[\exp \left(- \left(y - \sum_{k=1}^{m_*} a_k^* g_k(z_k) \right)^2 / (2\Delta) \right) \right]. \quad (48)$$

(49)

Note that $Z \in \mathcal{C}^\infty$ and, applying the definition of the probabilist's Hermite polynomials, its j^{th} derivative reads

$$\frac{d^j}{dy^j} Z(y) = \frac{(-1)^j}{\sqrt{2\pi\Delta^{j+1}}} \mathbb{E}_\mathbf{z} \left[e^{-\left(y - \sum_{k=1}^{m_*} a_k^* g_k(z_k) \right)^2 / (2\Delta)} \text{He}_k \left(\frac{y - \sum_{k=1}^{m_*} a_k^* g_k(z_k)}{\sqrt{\Delta}} \right) \right]. \quad (50)$$

We now aim to approximate integrals of the type $\mathbb{E}_Y[h(Y)G_k(Y)]$, where $h : \mathbb{R} \rightarrow \mathbb{R}$ is bounded, that are involved in eq. (38). In particular, we derive a bound for

$$\mathcal{E}_k := \mathbb{E}[h(Y)G_k(Y)] - a_k^* \mathbb{E}_z[g_k(z)(z^2 - 1)] \int dy h(y) Z'(y). \quad (51)$$

In the following, we leverage the Taylor's expansion of the complex exponential, ensuring that, for all $\omega \in \mathbb{R}$, $k \in \mathbb{N}$, there exists a constant $c \in [0, \omega]$ such that³

$$R_k(\omega) := e^{i\omega} - \sum_{j=0}^k \frac{(i\omega)^j}{j!}, \quad R_k(\omega) = \frac{(i\omega)^{k+1}}{k!} \int_0^1 e^{i\omega t} (1-t)^k dt \quad (52)$$

In addition, we use the Fourier representation of the Gaussian density $(2\pi)^{-1/2}e^{-x^2/2} = (2\pi)^{-1} \int d\omega e^{i\omega x - \omega^2/2}$ and the identity

$$\frac{1}{2\pi} \int d\omega e^{i\omega x - \omega^2} (i\omega)^j = \frac{1}{2\pi} \frac{d^j}{dx^j} \int d\omega e^{i\omega x - \omega^2} = (-1)^j \frac{e^{-x^2/2}}{\sqrt{2\pi}} \text{He}_j(x). \quad (53)$$

Define the shorthand $\rho_k^{jj'} := \mathbb{E}_z[g_k^j(z)\text{He}_{j'}(z)]$, for $j, j' \in \{0, 1, 2\}$, which are non-zero and finite by Assumption 2.3. In order to simplify the following equations, let $\mathbb{E}_{\mathbf{z}_{\setminus k}}$ denote the expected value with respect to $\{z_h\}_{h \neq k}$ and $S_k(\mathbf{z}_{\setminus k}) := \sum_{h \neq k} a_h^* g_h(z_h)$. Then, we have

$$\mathcal{E}_k = \int dy h(y) \mathbb{E}_{\mathbf{z}} [\mathbb{P}(y|\mathbf{z})(z_k^2 - 1) - a_k^* \rho_k^{12} \partial_y \mathbb{P}(y|\mathbf{z})] \quad (54)$$

$$\stackrel{(53)}{=} \mathbb{E}_{\mathbf{z}_{\setminus k}} \frac{1}{2\pi} \int dy h(y) \int d\omega e^{i\omega(y - S_k(\mathbf{z}_{\setminus k})) - \omega^2 \Delta/2} \mathbb{E}_z [e^{-i\omega a_k^* g_k(z)} (z^2 - 1)] \quad (55)$$

$$+ \frac{a_k^* \rho_k^{12}}{2\pi} \mathbb{E}_{\mathbf{z}_{\setminus k}} \int dy h(y) \int d\omega (i\omega) e^{i\omega(y - S_k(\mathbf{z}_{\setminus k})) - \omega^2 \Delta/2} \mathbb{E}_z [e^{-i\omega a_k^* g_k(z)}] \quad (56)$$

$$= \frac{1}{2\pi} \mathbb{E}_{\mathbf{z}_{\setminus k}} \int dy h(y) \int d\omega e^{i\omega(y - S_k(\mathbf{z}_{\setminus k})) - \omega^2 \Delta/2} \underbrace{\mathbb{E}_z [(1 - i\omega a_k^* g_k(z) + R_1(\omega a_k^* g_k(z)))(z^2 - 1)]}_{0 - i\omega a_k^* \rho_k^{12} + \mathbb{E}_z [R_1(\omega a_k^* g_k(z))](z^2 - 1)} \quad (57)$$

$$+ \frac{a_k^* \rho_k^{12}}{2\pi} \mathbb{E}_{\mathbf{z}_{\setminus k}} \int dy h(y) \int d\omega (i\omega) e^{i\omega(y - S_k(\mathbf{z}_{\setminus k})) - \omega^2 \Delta/2} \mathbb{E}_z [1 + R_0(\omega a_k^* g_k(z))]. \quad (58)$$

After the cancellation of the terms in a_k^* , substituting the integral form of the remainder in eq. (52)

$$\mathcal{E}_k = \frac{(a_k^*)^2}{2\pi} \mathbb{E}_{\mathbf{z}} g_k(z_k) (z_k^2 - 1) \int_0^1 dt (1-t) \int dy h(y) \int d\omega (i\omega)^2 e^{i\omega(y - S_k(\mathbf{z}_{\setminus k})) - \omega^2 \Delta/2} e^{it\omega a_k^* g_k(z_k)} \quad (59)$$

$$+ \frac{(a_k^*)^2 \rho_k^{12}}{2\pi} \mathbb{E}_{\mathbf{z}} g_k(z_k) \int_0^1 dt \int dy h(y) \int d\omega (i\omega)^2 e^{i\omega(y - S_k(\mathbf{z}_{\setminus k})) - \omega^2 \Delta/2} e^{it\omega a_k^* g_k(z_k)} \quad (60)$$

$$\stackrel{(53)}{=} \frac{(a_k^*)^2}{\Delta \sqrt{2\pi \Delta}} \mathbb{E}_{\mathbf{z}} g_k^2(z_k) (z_k^2 - 1) \int_0^1 dt (1-t) \int dy h(y) e^{-(y - S_k(\mathbf{z}_{\setminus k}) + ta_k^* g_k(z_k))^2 / (2\Delta)} \text{He}_2 \left(\frac{y - S_k(\mathbf{z}_{\setminus k}) + ta_k^* g_k(z_k)}{\sqrt{\Delta}} \right) \quad (61)$$

$$+ \frac{(a_k^*)^2 \rho_k^{12}}{\Delta \sqrt{2\pi \Delta}} \mathbb{E}_{\mathbf{z}} g_k(z_k) \int_0^1 dt \int dy h(y) e^{-(y - S_k(\mathbf{z}_{\setminus k}) + ta_k^* g_k(z_k))^2 / (2\Delta)} \text{He}_2 \left(\frac{y - S_k(\mathbf{z}_{\setminus k}) + ta_k^* g_k(z_k)}{\sqrt{\Delta}} \right) \quad (62)$$

$$= \frac{(a_k^*)^2}{\Delta \sqrt{2\pi}} \mathbb{E}_{\mathbf{z}} g_k^2(z_k) (z_k^2 - 1) \int_0^1 dt (1-t) \int dy h \left(\sqrt{\Delta} y + S_k(\mathbf{z}_{\setminus k}) - ta_k^* g_k(z_k) \right) e^{-y^2/2} \text{He}_2(y) \quad (63)$$

$$+ \frac{(a_k^*)^2 \rho_k^{12}}{\Delta \sqrt{2\pi}} \mathbb{E}_{\mathbf{z}} g_k(z_k) \int_0^1 dt \int dy h \left(\sqrt{\Delta} y + S_k(\mathbf{z}_{\setminus k}) - ta_k^* g_k(z_k) \right) e^{-y^2/2} \text{He}_2(y). \quad (64)$$

³The following expression is obtained as the integral form of the remainder in Taylor's theorem applied to the real functions $\sin(\omega)$ and $\cos(\omega)$ in $e^{i\omega} = \cos(\omega) + i\sin(\omega)$.

Recalling that h is a bounded function, we obtain

$$|\mathcal{E}_k| \leq \sup_{y \in \mathbb{R}} |h(y)| \frac{(a_k^*)^2}{\Delta \sqrt{2\pi}} \int dy e^{-y^2/2} |\text{He}_2(y)| \left(\frac{\rho_k^{22}}{2} + \rho_k^{12} \rho_k^{10} \right). \quad (65)$$

Note that, by Assumption 2.3, the constants $\rho_k^{jj'}$ do not scale with k , therefore $|\mathcal{E}_k| = O((a_k^*)^2)$. We now look for $t > \tau$ and α that are solutions of eqs. (47). In particular, the oracle k -critical threshold in Appendix A.1 is a lower bound to the spectral one, therefore $\alpha_k^{\text{sp}} = \Omega(\alpha_k^{\text{oracle}})$ and diverges with k . The second equation of (47), due to the monotonicity of the RHS, implies that also the solution t must diverge with k . Using the bound we have derived for \mathcal{E}_k ,

$$\begin{cases} (\alpha_k^{\text{sp}})^{-1} = t^{-1} a_k^* \mathbb{E}_z[g_k(z)(z^2 - 1)] \int dy \mathcal{T}(y) Z'(y) + O(a_k^* t^{-2} + (a_k^*)^2 t^{-1}) \\ (\alpha_k^{\text{sp}})^{-1} = t^{-2} \mathbb{E}[\mathcal{T}(y)^2] + O(t^{-3}). \end{cases} \quad (66)$$

In the previous, we have used

$$\left| \int dy \left(\frac{\mathcal{T}(y) Z'(y)}{t - \mathcal{T}(y)} - t^{-1} \mathcal{T}(y) Z'(y) \right) \right| = t^{-2} \left| \int dy \frac{\mathcal{T}^2(y) Z'(y)}{1 - \mathcal{T}(y)/t} \right| \quad (67)$$

$$\leq t^{-2} \sup_{y \in \mathbb{R}} \left(\frac{\mathcal{T}^2(y)}{1 - \mathcal{T}(y)/t} \right) \int dy |Z'(y)| \quad (68)$$

$$\stackrel{(50)}{=} t^{-2} \sup_{y \in \mathbb{R}} \left(\frac{\mathcal{T}^2(y)}{1 - \mathcal{T}(y)/t} \right) \int dy \frac{e^{-y^2/2}}{\sqrt{2\pi\Delta}} |y| = O(t^{-2}), \quad (69)$$

where, for t sufficiently large, the supremum is bounded by a constant independent of t . The system (66) is thereby solved for

$$t^{-1} = \Theta(a_k^*), \quad \alpha_k^{\text{sp}} = \Theta(\alpha_k^{\text{oracle}}). \quad (70)$$

We can now derive the scaling laws for the spectral weighted mean-squared error. Taking $\alpha \gg \alpha_k^{\text{sp}}$, for k large enough, the solution t_k of eq. (45) scales as $t_k = \Theta(\alpha a_k^*)$. As a consequence of Theorem 4.2 in Kovačević et al. (2025), specialized in our setting – where we can exploit the diagonality of $\mathbf{G}(y)$, we have that the overlap between the eigenvector \mathbf{v}_k corresponding to the eigenvalue λ_k^T , and the true signal \mathbf{w}_h^* , converges, in the high-dimensional limit, to an overlap

$$m_{hk}^2 := \frac{1}{d^2} \langle \mathbf{w}_h^*, \mathbf{v}_k \rangle^2 = \delta_{kh} \frac{\zeta'_\alpha(t_k)}{\zeta'_\alpha(t_k) + \frac{d}{dt} R_k(t_k)}, \quad (71)$$

where $R_k(t) = \mathbb{E}[z_k^2 \mathcal{T}(y)/(t - \mathcal{T}(y))]$. For $\alpha \gg \alpha_k^{\text{sp}}$ we have that $t_k \gg 1$ and eq. (45) is solved by $t_k = \Theta(a_k^* \alpha)$. Putting all together

$$m_{hk}^2 = \delta_{kh} \left(1 - \Theta \left(\frac{(\alpha_k^*)^{-2}}{\alpha} \right) \right). \quad (72)$$

Recall that

$$\text{mse}_k(\mathbf{v}_k) = \frac{1}{d^2} \mathbb{E} [\|\mathbf{v}_k \mathbf{v}_k^\top\|_{\text{F}}^2 + \|\mathbf{w}_k^* \mathbf{w}_k^{*\top}\|_{\text{F}}^2 - 2 \langle \mathbf{w}_k^*, \mathbf{v}_k \rangle^2] \rightarrow 2(1 - m_{kk}^2). \quad (73)$$

By repeating computations analogous to the ones in Appendix A.1, one finds, setting $\hat{\mathbf{W}} = (\mathbf{v}_1, \dots, \mathbf{v}_r)^\top$,

$$\text{MMSE}_\gamma(\hat{\mathbf{W}} := (\hat{\mathbf{W}}^{\text{sp}}, \mathbf{0}_{(m_* - r) \times d})) = \Theta(\text{MMSE}_\gamma^{\text{oracle}}), \quad (74)$$

which proves Theorem 3.2 and 3.6.

B Proof of Theorem 3.8

In this section we prove Theorem 3.8, stating that a two-layer neural network, trained according to Algorithm 1, can achieve an excess risk bottlenecked by the information-theoretic error on the recovery of the representations \mathbf{W}_* . Denote $\hat{\mathbf{W}}^{\text{sp}} \in \mathbb{R}^{r \times d}$ the spectral estimator defined in 3.3. In Appendix A.2 we have shown that each

column k correlates with the signal component \mathbf{w}_k^* only, with squared overlap $m_k = 1 - \Theta((\alpha_k^*)^{-2}/\alpha)$. Denote \mathbf{v}_k as the k^{th} column of the spectral estimator and $\eta_k^2 := (\alpha_k^*)^2/\alpha \ll 1$. Up to negligible corrections $O(\eta_k^2)$

$$\mathbf{w}_k^* = \mathbf{v}_k + \eta_k \boldsymbol{\xi}_k, \quad (75)$$

with $\boldsymbol{\xi}_k$ a unit vector orthogonal to all $\{\mathbf{v}_h\}_{h \in [r]}$. Given a covariate $\mathbf{x} \in \mathbb{R}^d$, define the projected inputs $\mathbf{s} \in \mathbb{R}^r$ such that $s_k = \langle \mathbf{v}_k, \mathbf{x} \rangle$, $k \in [r]$. The first layer pre-activations are given by

$$\mathbf{W}\mathbf{x} = \mathbf{Z}\hat{\mathbf{W}}^{\text{sp}}\mathbf{x} = \mathbf{Z}\mathbf{s}. \quad (76)$$

Similarly, up to negligible corrections $O(\eta_k^2)$, the target function

$$f_*(\mathbf{x}) = \sum_{k=1}^r a_k^* g_k(s_k + \eta_k \langle \boldsymbol{\xi}_k, \mathbf{x} \rangle) + \sum_{k=r+1}^{m_*} a_k^* g_k(\langle \mathbf{w}_k^*, \mathbf{x} \rangle) \quad (77)$$

$$= \sum_{k=1}^r a_k^* g_k(s_k) + \sum_{k=1}^r a_k^* g'_k(s_k) \eta_k \langle \boldsymbol{\xi}_k, \mathbf{x} \rangle + \sum_{k=r+1}^{m_*} a_k^* g_k(\langle \mathbf{w}_k^*, \mathbf{x} \rangle). \quad (78)$$

Due to the orthogonality between $\boldsymbol{\xi}_k$ and \mathbf{v}_h , and $\mathbf{x} \sim \mathcal{N}(\mathbf{0}, d^{-1}\mathbf{I}_d)$, for any $h, k \in [r]$, the variables $\langle \mathbf{x}, \boldsymbol{\xi}_k \rangle$ and s_h are independent centered Gaussian variables. With respect to the projected input space, the effective target function is

$$f_*^{\text{eff}}(\mathbf{s}) := \mathbb{E}[f_*(\mathbf{x})|\mathbf{s}] = \sum_{i=1}^r a_k^* g_k(s_k). \quad (79)$$

Then, the readout training in Algorithm 1 corresponds to random feature ridge regression [Rahimi and Recht \(2007\)](#) with weights $\mathbf{Z} = (\mathbf{z}_1, \dots, \mathbf{z}_p)^\top$ on the projected covariates $\mathbf{s}_i = \hat{\mathbf{W}}^{\text{sp}}\mathbf{x}_i^{(2)}$, $i \in [n]$, where $\{\mathbf{x}_i^{(2)}\}_{i \in [n]}$ are the covariates in the dataset \mathcal{D}_2 :⁴

$$\hat{\mathbf{a}} = \arg \min_{\mathbf{a} \in \mathbb{R}^p} \frac{1}{2n} \sum_{i=1}^n \left(y_i - \sum_{j=1}^p a_j \sigma(\langle \mathbf{z}_j, \mathbf{s}_i \rangle) \right)^2 + \frac{\lambda}{2} \|\mathbf{a}\|^2 \quad (80)$$

Since σ is bounded and continuous, and the effective label noise is sub-exponential, as it is given by a polynomial of Gaussian random variables, we can apply Theorem 1 in [Rudi and Rosasco \(2017\)](#)⁵, choosing $p = \omega(n^{1/2})$, $\lambda = \Theta(n^{-1/2})$, so that we obtain that the risk eq. (11) $R(\hat{\mathbf{a}}, \mathbf{W})$ satisfies

$$R(\hat{\mathbf{a}}, \mathbf{W}) - R_{f_{\mathcal{H}}} = O(n^{-1/2}), \quad (81)$$

where, given the *reproducing kernel Hibert space* (RKHS) \mathcal{H} associated to the kernel $K(\mathbf{s}, \mathbf{s}') = \mathbb{E}_{\mathbf{z}, b}[\sigma(\mathbf{s}^\top \mathbf{s} + b)\sigma(\mathbf{s}'^\top \mathbf{s}' + b)]$,

$$R_{f_{\mathcal{H}}} = \min_{f \in \mathcal{H}} \mathbb{E}_{y, \mathbf{s}}[(f(\mathbf{s}) - y)^2]. \quad (82)$$

Such irreducible risk is lower-bounded by

$$R_* = \mathbb{E}[(f_*^{\text{eff}}(\mathbf{s}) - y)^2] \quad (83)$$

$$= \mathbb{E} \left[\left(\sum_{k=1}^r a_k^* g'_k(s_k) \eta_k \langle \boldsymbol{\xi}_k, \mathbf{x} \rangle + \sum_{k=r+1}^{m_*} a_k^* g_k(\langle \mathbf{w}_k^*, \mathbf{x} \rangle) \right)^2 \right] \quad (84)$$

$$= \Theta \left(\sum_{k=1}^r (a_k^*)^2 \eta_k^2 + \sum_{k=r+1}^{m_*} (a_k^*)^2 \right) = \Theta(\text{MMSE}_\gamma), \quad (85)$$

⁴In order to simplify the notation, we denote the labels in \mathcal{D}_2 as $y_i := y_i^{(2)}$.

⁵Note that the assumption of bounded outputs in Theorem 1 is relaxed in the Appendix of [Rudi and Rosasco \(2017\)](#), including settings with sub-exponential noise, see Assumption 4. Further, the analysis in this work allows for a more refined error rate in our setting. However, the result we obtain is already subleading with respect to the rates in Theorem 3.2.

where, as for the spectral method mean-squared error, the two terms correspond to the approximation error of learned features and underfitting of unlearned ones. If $f_\star^{\text{eff}} \in \mathcal{H}$, the argument is complete. By assumption, the function σ allows for a decomposition in Hermite polynomials

$$\sigma(z) = \sum_{\beta \geq 0} \frac{\sigma_\beta}{\beta!} \text{He}_\beta(z), \quad \sigma_\beta := \frac{1}{\beta!} \mathbb{E}_z[\text{He}_\beta(z)\sigma(z)]. \quad (86)$$

Further, being bounded, it cannot be a polynomial of finite degree, as there is no β_0 such that $\sigma_\beta = 0$ for all $\beta \geq \beta_0$, excluding the trivial case of constant functions. Considering the Taylor expansion of Hermite polynomials

$$\text{He}_\beta(z + b) = \sum_{\zeta=0}^{\beta} \binom{\beta}{\zeta} b^{\beta-\zeta} \text{He}_\zeta(z), \quad (87)$$

with $\binom{\beta}{\zeta} = \frac{\beta!}{\zeta!(\beta-\zeta)!}$, we find that the kernel K is given by

$$K(\mathbf{s}, \mathbf{s}') = \mathbb{E}_{\mathbf{z}, b}[\sigma(\mathbf{z}^\top \mathbf{s} + b)\sigma(\mathbf{z}^\top \mathbf{s}' + b)] \quad (88)$$

$$= \mathbb{E}_{\mathbf{z}, b} \sum_{\beta, \beta' \geq 0} \sum_{\zeta=0}^{\beta} \sum_{\zeta'=0}^{\beta'} \frac{\sigma_\beta \sigma_{\beta'}}{\zeta! \zeta'! (\beta - \zeta)! (\beta' - \zeta')!} b^{\beta-\zeta} b^{\beta'-\zeta'} \text{He}_\zeta(\langle \mathbf{z}, \mathbf{s} \rangle) \text{He}_{\zeta'}(\langle \mathbf{z}, \mathbf{s}' \rangle) \quad (89)$$

By Proposition 11.31 in [O'Donnell \(2014\)](#),

$$K(\mathbf{s}, \mathbf{s}') = \mathbb{E}_b \sum_{\beta, \beta' \geq 0} \sum_{\zeta=0}^{\min(\beta, \beta')} \frac{\sigma_\beta \sigma_{\beta'}}{\zeta! (\beta - \zeta)! (\beta' - \zeta)!} b^{\beta+\beta'-2\zeta} \frac{\langle \mathbf{s}, \mathbf{s}' \rangle^\zeta}{r^\zeta} \quad (90)$$

$$= \mathbb{E}_b \sum_{\zeta=0}^{\infty} \sum_{\beta, \beta' \geq \zeta} \frac{\sigma_\beta \sigma_{\beta'}}{\zeta! (\beta - \zeta)! (\beta' - \zeta)!} b^{\beta+\beta'-2\zeta} \frac{\langle \mathbf{s}, \mathbf{s}' \rangle^\zeta}{r^\zeta} \quad (91)$$

$$= \underbrace{\sum_{\zeta=0}^{\infty} \mathbb{E}_b \left(\sum_{\beta \geq \zeta} \frac{\sigma_\beta}{\zeta! (\beta - \zeta)!} b^{\beta-\zeta} \right)^2 \frac{\langle \mathbf{s}, \mathbf{s}' \rangle^\zeta}{r^\zeta}}_{\text{bracketed term}} \quad (92)$$

The bracketed term is always strictly positive as the polynomial $\sum_{\beta \geq \zeta} \frac{\sigma_\beta}{\zeta! (\beta - \zeta)!} b^{\beta-\zeta}$ in b cannot be identically zero. In fact, this would require that $\sigma_\beta = 0$ for all $\beta > \zeta$, which would imply that σ is a polynomial, contradicting the hypothesis of boundedness. Expanding the term $\langle \mathbf{s}, \mathbf{s}' \rangle$, it follows that the kernel admits a decomposition as $K(\mathbf{s}, \mathbf{s}') = \Phi(\mathbf{s})^\top \Phi(\mathbf{s}')$, where Φ is a feature map with components given by multivariate monomials $\lambda_\beta s_1^{\beta_1} \dots s_r^{\beta_r}$, for some $\lambda_\beta > 0$ for all degrees $|\beta|$. Theorem 4.21 in [Christmann and Steinwart \(2008\)](#) readily implies that the RKHS of K includes all finite degree polynomials, completing our argument.

C Useful results on single-index models

In this section we present various results applied in the derivation of the lower bound to MMSE_γ in Appendix [A.1](#). In particular, we focus on the following single-index model setting.

Definition C.1. Let $\mathbf{w}^* \sim \mathcal{N}(\mathbf{0}_d, \mathbf{I}_d)$, $g : \mathbb{R} \rightarrow \mathbb{R}$ satisfy Assumption [2.3](#). Consider the supervised learning problem of estimating \mathbf{w}^* from n i.i.d. observations $\mathcal{D} = \{(\mathbf{x}_i, y_i) \in \mathbb{R}^{d \times 1} : i \in [n]\}$ generated as

$$\mathbf{x}_i \sim \mathcal{N}(\mathbf{0}, \mathbf{I}_d), \quad y_i = \sqrt{\lambda} g(\langle \mathbf{x}_i, \mathbf{w}^* \rangle) + \xi_i, \quad (93)$$

where $\lambda \geq 0$ is the signal-to-noise ratio (SNR) and $\xi_i \sim \mathcal{N}(0, 1)$ is additive noise.

Given an estimator $\hat{\mathbf{w}}$ of \mathbf{w}^* that is a function of the dataset, we evaluate its estimation error using the following matrix-MMSE:

$$\text{mse}(\mathbf{w}) := \frac{1}{d^2} \mathbb{E}[\|\mathbf{w}\mathbf{w}^\top - \mathbf{w}^*\mathbf{w}^{*\top}\|_F^2], \quad (94)$$

where \mathbb{E} computes the expected value with respect to the joint distributions of \mathcal{D} and \mathbf{w}_* . A lower bound to this quantity is given by the following optimal matrix-MSE

$$\text{mmse} := \frac{1}{d^2} \mathbb{E} [\|\mathbb{E}[\mathbf{w}\mathbf{w}^T | \mathcal{D}] - \mathbf{w}^* \mathbf{w}^{*\top}\|_F^2] = \arg \min_{\mathbf{Q} \in \mathbb{R}^{d \times d}} \mathbb{E} [\|\mathbf{Q} - \mathbf{w}^* \mathbf{w}^{*\top}\|_F^2]. \quad (95)$$

Intuitively, such optimal estimation error decreases with the SNR.

Lemma C.2. *In the setting defined in C.1, the optimal matrix-MSE satisfies*

$$\frac{\partial}{\partial \lambda} \text{mmse} < 0. \quad (96)$$

Proof. The proof follows from direct computation. We provide here a condensed derivation.

$$\text{mmse} = \mathbb{E} [\|\mathbf{w}\mathbf{w}^T\|_F^2] - \mathbb{E}_{\mathbf{y}} [\|\mathbb{E}[\mathbf{w}\mathbf{w}^T | \mathbf{y}]\|_F^2]. \quad (97)$$

Since the first term is independent of λ , it suffices to show that the second term is non-decreasing. Let us denote the posterior mean as $\langle \mathbf{w}\mathbf{w}^T \rangle_\lambda \equiv \mathbb{E}[\mathbf{w}\mathbf{w}^T | \mathbf{y}]$. We compute its derivative with respect to λ :

$$\frac{d}{d\lambda} \mathbb{E}_{\mathbf{y}} [\|\langle \mathbf{w}\mathbf{w}^T \rangle_\lambda\|_F^2] = \int d\mathbf{y} \frac{\partial}{\partial \lambda} (\mathbb{P}(\mathbf{y}) \|\langle \mathbf{w}\mathbf{w}^T \rangle_\lambda\|_F^2). \quad (98)$$

Using the explicit form of $\mathbb{P}(\mathbf{y} | \mathbf{w}) \propto \exp\left(-\frac{1}{2}\|\mathbf{y} - \sqrt{\lambda}g(\mathbf{X}\mathbf{w})\|^2\right)$, the derivative $\partial_\lambda \ln \mathbb{P}(\mathbf{y})$ introduces terms involving $\mathbf{y}^T \langle g(\mathbf{X}\mathbf{w}) \rangle_\lambda$. We handle these terms via the multivariate Stein's Lemma (corresponding to integration by parts), which states that for the Gaussian measure, $\mathbb{E}_{\mathbf{y}}[\mathbf{y}^T \mathbf{f}(\mathbf{y})] = \mathbb{E}_{\mathbf{y}}[\text{Tr}(\nabla \mathbf{f}) + \sqrt{\lambda} \langle h(\mathbf{X}\mathbf{w}) \rangle_\lambda^T \mathbf{f}]$.

Applying this identity results in cancellations of the lower-order terms. The surviving term is proportional to the gradient of the estimator with respect to the observations $\nabla_{\mathbf{y}} \langle \mathbf{w}\mathbf{w}^T \rangle_\lambda = \sqrt{\lambda} \text{Cov}(\mathbf{w}\mathbf{w}^T, g(\mathbf{X}\mathbf{w}) | \mathbf{y})$. Therefore,

$$\frac{d}{d\lambda} \mathbb{E}_{\mathbf{y}} [\|\langle \mathbf{w}\mathbf{w}^T \rangle_\lambda\|_F^2] = \mathbb{E}_{\mathbf{y}} [\|\text{Cov}(\mathbf{w}\mathbf{w}^T, g(\mathbf{X}\mathbf{w}) | \mathbf{y})\|_F^2] \implies \frac{\partial}{\partial \lambda} \text{mmse} < 0. \quad (99)$$

□

We now consider the high-dimensional limit $n, d \rightarrow \infty$ with fixed ratio $\alpha = n/d$, referred to as the sample complexity. The following theorem specializes Theorems 1 and 2 of [Barbier et al. \(2019\)](#) to the setting of interest.

Theorem C.3 ([Barbier et al. \(2019\)](#)). *Consider the setting defined in C.1. Then, in the limit $n, d \rightarrow \infty$, with fixed ratio $n/d = \alpha$,*

$$\frac{1}{d^2} \mathbb{E} \|\mathbf{w}^* \mathbf{w}^{*\top} - \mathbb{E}[\mathbf{w}\mathbf{w}^T | \mathcal{D}]\|_F^2 \rightarrow 1 - m^2, \quad (100)$$

and, given $\mathbf{w} \sim \mathbb{P}(\cdot | \mathcal{D})$,

$$\frac{1}{d} |\mathbf{w}^T \mathbf{w}^*| \xrightarrow{\mathbb{P}} m, \quad (101)$$

where $m = m(\alpha)$ is the maximizer of

$$\sup_{m \in [0, 1]} f_{\text{RS}}(m), \quad f_{\text{RS}}(m) := \{m + \log(1 - m) + 2\alpha \Psi_{\text{out}}(m)\}, \quad (102)$$

$$\Psi_{\text{out}}(m; \lambda) := \mathbb{E}_{W, V, Y} \log \mathbb{E}_{w \sim \mathcal{N}(0, 1)} [\mathbb{P}(Y | \sqrt{m}V + \sqrt{1 - m}w)], \quad (103)$$

with $V, W \sim \mathcal{N}(0, 1)$, $Y \sim \mathbb{P}(\cdot | \sqrt{m}V + \sqrt{1 - m}W)$.

As a direct consequence of the theorem, the information-theoretic weak recovery threshold α^{IT} is the smallest sample complexity α such that the maximizer of the free entropy eq. (102) is $m \neq 0$. Equivalently, α^{IT} is the smallest α such that $\text{mmse} < 1$. Lemma C.2 readily implies that $\alpha^{\text{IT}} = \alpha^{\text{IT}}(\lambda)$ is decreasing with the SNR.

Finally, we characterize the IT weak recovery threshold in the limit of small SNR. By expanding eq. (103) around $\lambda = 0$, we derive the following Corollary.

Corollary C.4 (IT weak recovery threshold in the large noise regime). *Consider the setting of Theorem C.3. Then, in the limit $\lambda \rightarrow 0$, the information theoretic weak-recovery threshold satisfies*

$$\alpha^{\text{IT}} = \Theta(\lambda^{-1}) \quad (104)$$

and, for $\alpha \rightarrow \infty$, and fixed λ the optimal matrix-MSE scales as

$$\text{mmse} = O\left(\frac{1}{\lambda\alpha}\right). \quad (105)$$

Proof. For a fixed $m \in [0, 1]$), consider the function

$$F(\kappa) := \mathbb{E}_{W,V,Y} \log \mathbb{E}_{w \sim \mathcal{N}(0,1)} [\exp(y - \kappa g(\sqrt{m}V + \sqrt{1-m}w))], \quad (106)$$

with $V, W \sim \mathcal{N}(0, 1)$, $Y \sim \mathcal{N}(\kappa g(\sqrt{m}V + \sqrt{1-m}W), 1)$. It is straightforward to show, by a change of variable $Y \rightarrow -Y$, that F is even. Note that, up to constant terms in m , $F(\kappa) = \Psi_{\text{out}}(m; \kappa^2)$.

Furthermore, as a consequence of Taylor's theorem, there exists constant $\hat{\kappa} \in [0, \kappa]$, such that $F(\kappa) = F(0) + \frac{1}{2}F''(0)\kappa^2 + \frac{1}{24}F^{(4)}(\hat{\kappa})\kappa(\kappa - \hat{\kappa})^3$. By Lemma C.5, there exists a finite $C > 0$, constant in κ and m , such that

$$\left| \frac{1}{24}F^{(4)}(\hat{\kappa})\kappa(\kappa - \hat{\kappa})^3 \right| < C\kappa^4. \quad (107)$$

Define the auxiliary function

$$Z(\kappa, v, u, y) := \frac{1}{\sqrt{2\pi}} \mathbb{E}_w [\exp(-(y - \kappa(g(\sqrt{m}v + \sqrt{1-m}w) - g(\sqrt{m}v + \sqrt{1-m}u))^2/2)]. \quad (108)$$

In particular, $Z(0, v, u, y) = (2\pi)^{-1/2}e^{-y^2/2}$ and, applying the definition of the probabilist's Hermite polynomials, for all $j \in \mathbb{N}$, using the shorthand $g_u = g(\sqrt{m}v + \sqrt{1-m}u)$

$$\frac{\partial^j}{\partial \kappa^j} Z(\kappa, v, u, y) = \frac{1}{\sqrt{2\pi}} \mathbb{E}_w \left[e^{-(y - \kappa(g_w - g_u))^2/2} \text{He}_j(y - \kappa(g_w - g_u)) \frac{(g_w - g_u)^j}{j!} \right] \quad (109)$$

we have, after a change of variable $Y \rightarrow Y + \kappa g\sqrt{m}V + \sqrt{1-m}W$, that $F(\kappa) = \mathbb{E}_{V,W,Y}[\log Z(\kappa, V, W, Y)]$ for $Y \sim \mathcal{N}(0, 1)$ and

$$F''(0) = \mathbb{E}_{V,W,Y} \left[\frac{Z''(0, V, W, Y)}{Z(0, V, W, Y)} - \left(\frac{Z'(0, V, W, Y)}{Z(0, V, W, Y)} \right)^2 \right] \quad (110)$$

$$= \mathbb{E}_Y[Y](\mathbb{E}_{V,W}[g_w] - \mathbb{E}_{V,w}[g_w]) - \frac{1}{2}\mathbb{E}_Y[(Y^2 - 1)](\mathbb{E}_{V,W}[g_w^2] + \mathbb{E}_{V,W}[g_w^2] - 2\mathbb{E}_{V,W,w}[g_w g_w]) \quad (111)$$

$$= 0 - \mathbb{E}_{z \sim \mathcal{N}(0,1)}[g^2(z)] + \mathbb{E}_{(z_1, z_2) \sim \mathcal{N}(\mathbf{0}_2, \mathbf{C})}[g(z_1)g(z_2)] \quad (112)$$

with

$$\mathbf{C} = \begin{pmatrix} 1 & m \\ m & 1 \end{pmatrix}. \quad (113)$$

In the above we used

$$\mathbb{E}_{V,W}[g_w^2] = \mathbb{E}_{W,V}[g^2(\sqrt{m}V + \sqrt{1-m}W)] = \mathbb{E}_z[g^2(z)], \quad (114)$$

$$\mathbb{E}_{V,W,W}[g_w g_W] = \mathbb{E}_V[\mathbb{E}_W[g(\sqrt{m}V + \sqrt{1-m}W)]\mathbb{E}_w[g(\sqrt{m}V + \sqrt{1-m}w)]] \quad (115)$$

$$= \mathbb{E}_{(z_1, z_2) \sim \mathcal{N}(\mathbf{0}_2, \mathbf{C})}[g(z_1)g(z_2)]. \quad (116)$$

Therefore, up to constant terms in m ,⁶

$$\Psi_{\text{out}}(m; \lambda) = F(\sqrt{\lambda}) = \text{const} + \frac{\lambda}{2} \mathbb{E}_{(z_1, z_2) \sim \mathcal{N}(\mathbf{0}_2, \mathbf{C})}[g(z_1)g(z_2)] + O(\lambda^2). \quad (117)$$

⁶Recall that, by Lemma C.5, the correction $O(\lambda^2)$ is uniform in $m \in [0, 1]$.

Assumption 2.3 ensures that g can be decomposed in the Hermite basis as

$$g(z) = \sum_{k \geq 0} \frac{c_k}{k!} \text{He}_k(z), \quad c_k := \frac{1}{k!} \mathbb{E}_{z \sim \mathcal{N}(0,1)} [g(z) \text{He}_k(z)]. \quad (118)$$

Leveraging Proposition 11.31 in O'Donnell (2014),

$$\mathbb{E}_{(z_1, z_2) \sim \mathcal{N}(\mathbf{0}_2, \mathbf{C})} [g(z_1)g(z_2)] = \sum_{k \geq 0} \frac{c_k^2}{k!} m^k \in [0, \mathbb{E}_z [g^2(z)]], \quad (119)$$

which is a non-decreasing function of $m \in [0, 1]$. Note that, since g has generative exponent 2, and $\mathbb{E}_z [g(z)] = 0$, we have that $c_0 = c_1 = 0$ necessarily. Moreover, by Assumption 2.3, $c_2 \neq 0$ and bounded. Hence, we are interested in maximizing the quantity⁷

$$f_{\text{RS}}(m) := m + \log(1 - m) + \alpha \lambda \sum_{k \geq 2} \frac{c_k^2}{k!} m^k + O(\alpha \lambda^2) \quad (120)$$

$$= \frac{1}{2} (\alpha \lambda c_2^2 - 1) m^2 + \sum_{k > 2} \left(\frac{\alpha \lambda}{k!} c_k^2 - \frac{1}{k} \right) m^k + O(\alpha \lambda^2), \quad (121)$$

where we have expanded $\log(1 - m)$. For $\alpha > \lambda^{-1} c_2^{-2}$, $m = 0$ is a minimum of the free entropy, therefore $\alpha^{\text{IT}} \leq \lambda^{-1} c_2^{-2}$. Denote

$$D := \inf_{m \in (0,1]} \frac{-m - \log(1 - m)}{\sum_k \frac{c_k^2}{k!} m^k}, \quad (122)$$

which is strictly positive and well-defined. Note that

$$\lim_{m \rightarrow 0^+} \frac{-m - \log(1 - m)}{\sum_k \frac{c_k^2}{k!} m^k} = c_2^{-2} \implies \frac{1}{\mathbb{E}_z [g^2(z)]} \leq D \leq c_2^{-2} = \frac{1}{\mathbb{E}_z [g''(z)]}. \quad (123)$$

Then, for all $\alpha < D\lambda^{-1}$, $f(m \neq 0) < f(0) = 0$, i.e. $m = 0$ is the global maximizer and

$$D \leq \alpha^{\text{IT}} \lambda \leq c_2^{-2} \implies \alpha^{\text{IT}} = \Theta(\lambda^{-1}), \quad (124)$$

For the second result, we first consider the setting $\lambda \rightarrow 0$ and $\alpha \rightarrow \infty$, with $\alpha \gg \lambda$. There exists a non-zero maximizer m , which satisfies⁸

$$\frac{d}{dm} f_{\text{RS}}(m) \stackrel{!}{=} 0 \implies \frac{1}{1 - m} = \alpha \lambda \sum_{k \geq 2} \frac{c_k^2}{k!} m^{k-2} \implies \sum_{k \geq 2} \frac{c_k^2}{k!} (m^{k-2} - m^{k-1}) = \frac{1}{\alpha \lambda}, \quad (125)$$

The equation is solved by $m = 1 - \Theta(\frac{1}{\alpha \lambda})$. Theorem C.3 implies that, in this regime, $\text{mmse}(\lambda) = \Theta((\alpha \lambda)^{-1})$. Together Lemma C.2, the result for arbitrary λ is proved. \square

In the proof of the Corollary we have used the following lemma.

Lemma C.5. *Let $m \in [0, 1]$ and consider the function $Z : \mathbb{R}^4 \rightarrow \mathbb{R}$*

$$Z(\kappa, v, w, y) := \frac{1}{\sqrt{2\pi}} \mathbb{E}_{U \sim \mathcal{N}(0,1)} \left[e^{-\left(y - \kappa(g(\sqrt{m}v + \sqrt{1-m}U) - g(\sqrt{m}v + \sqrt{1-m}w)) \right)^2 / 2} \right]. \quad (126)$$

Then, for all $k \in \mathbb{N}$, there exists a universal constant C_k such that

$$\mathbb{E}_{W, V, Y} \left| \frac{\partial^k}{\partial \kappa^k} \log Z(\kappa, V, W, Y) \right| < C_k. \quad (127)$$

with $V, W, Y \sim \mathcal{N}(0, 1)$.

⁷Note that we are neglecting constant terms with respect to m .

⁸In the following we retain the leading terms in the free entropy expansion.

Proof. In order to simplify the notation, given $V \sim \mathcal{N}(0, 1)$, define the shorthand $g_w = g(\sqrt{m}V + \sqrt{1-m}w)$. By Faà di Bruno's formula, using the shorthand $Z = Z(\kappa, v, w, y)$ we have that

$$\frac{\partial^k}{\partial \kappa^k} \log Z = \sum_{\mathbf{m}: \sum_j j m_j = k} \frac{k!}{m_1! \dots m_k!} \frac{(-1)^{|\mathbf{m}|}}{|\mathbf{m}| Z^{|\mathbf{m}|}} \prod_{j=1}^k \left(\frac{\partial_\kappa^{(j)} Z}{j!} \right)^{m_j}, \quad (128)$$

$$= \sum_{\mathbf{m}: \sum_j j m_j = k} \frac{k!}{m_1! \dots m_k!} \frac{(-1)^{|\mathbf{m}|}}{|\mathbf{m}|} \prod_{j=1}^k \left(\frac{\partial_\kappa^{(j)} Z}{j! Z} \right)^{m_j}, \quad (129)$$

with $\mathbf{m} \in \mathbb{N}^k$ and $|\mathbf{m}| = \sum_j m_j$. Therefore, applying the triangle inequality and Holder's inequality

$$\mathbb{E} \left| \frac{\partial^k}{\partial \kappa^k} \log Z \right| \leq \sum_{\mathbf{m}: \sum_j j m_j = k} \frac{k!}{m_1! \dots m_k!} \frac{(-1)^{|\mathbf{m}|}}{|\mathbf{m}|} \prod_{j=1}^k \left(\mathbb{E} \left| \frac{\partial_\kappa^{(j)} Z}{j! Z} \right|^{km_j} \right)^{1/k}. \quad (130)$$

Since the sum runs over a finite number of k -tuples, the problem can be reduced to showing the finiteness of the quantities

$$\mathbb{E}_{V,W,Y} \left| \frac{\partial_\kappa^j Z(\kappa, V, W, Y)}{Z(\kappa, V, W, Y)} \right|^p, \quad p \in \mathbb{N} \quad (131)$$

Recalling the definition of the probabilist's Hermite polynomials:

$$\frac{1}{Z} \frac{\partial^j}{\partial \kappa^j} Z = \frac{1}{Z \sqrt{2\pi}} \mathbb{E}_U \left[e^{-(y+\kappa(g_W - g_U))^2/2} \text{He}_j(y + \kappa(g_W - g_U)) \frac{(g_W - g_U)^j}{j!} \right] \quad (132)$$

$$= \mathbb{E}_{U \sim \mathbb{Q}} \left[\text{He}_j(y + \kappa(g_W - g_U)) \frac{(g_W - g_U)^j}{j!} \right], \quad (133)$$

where we have defined the probability density function

$$d\mathbb{Q}(U) = \frac{\exp(-U^2/2 - (y + \kappa(g_W - g_U))^2/2)}{\mathbb{E}_{U \sim \mathcal{N}(0,1)} [\exp(-U^2/2 - (y + \kappa(g_W - g_U))^2/2)]} dU. \quad (134)$$

Applying Jensen's inequality to the convex function $|\cdot|^p$ we obtain

$$\mathbb{E}_{V,W,Y} \left| \frac{\partial_\kappa^j Z(\kappa, V, W, Y)}{Z(\kappa, V, W, Y)} \right|^p \quad (135)$$

$$\leq \mathbb{E}_{V,W,Y} \mathbb{E}_{U \sim \mathbb{Q}} \left| \text{He}_j(y + \kappa(g_W - g_U)) \frac{(g_W - g_U)^j}{j!} \right|^p \quad (136)$$

using the change of variable $y \rightarrow y - \kappa g_W$

$$= \mathbb{E}_V \int dy \mathbb{E}_W \frac{e^{-(y-\kappa g_W)^2/2}}{\sqrt{2\pi}} \frac{\mathbb{E}_{U \sim \mathcal{N}(0,1)} \left[e^{-(y-\kappa g_U)^2/2} \left| \text{He}_j(y - \kappa g_U) \frac{(g_W - g_U)^j}{j!} \right|^p \right]}{\mathbb{E}_U [e^{-(y-\kappa g_U)^2/2}]}, \quad (137)$$

$$\leq 2^{jp-1} \mathbb{E}_V \int dy \mathbb{E}_W \frac{e^{-(y-\kappa g_W)^2/2}}{\sqrt{2\pi}} \frac{\mathbb{E}_{U \sim \mathcal{N}(0,1)} \left[e^{-(y-\kappa g_U)^2/2} |\text{He}_j(y - \kappa g_U)|^p \frac{|g_W|^{jp} + |g_U|^{jp}}{j!^p} \right]}{\mathbb{E}_U [e^{-(y-\kappa g_U)^2/2}]}, \quad (138)$$

$$= \frac{2^{jp-1}}{j!^p} \underbrace{\mathbb{E}_V \int dy \mathbb{E}_{W \sim \mathbb{Q}} \left[|g_W|^{jp} \right] \frac{\mathbb{E}_{U \sim \mathcal{N}(0,1)} \left[e^{-(y-\kappa g_U)^2/2} |\text{He}_j(y - \kappa g_U)|^p \right]}{\sqrt{2\pi}}}_{=: T_1} \quad (139)$$

$$\frac{2^{jp-1}}{j!} \underbrace{\mathbb{E}_V \int dy \mathbb{E}_U \frac{e^{-(y-\kappa g_U)^2/2}}{\sqrt{2\pi}} \frac{\mathbb{E}_{U \sim \mathcal{N}(0,1)} \left[e^{-(y-\kappa g_U)^2/2} |\text{He}_j(y - \kappa g_w)|^p |g_w|^{jp} \right]}{\mathbb{E}_U [e^{-(y-\kappa g_U)^2/2}]}}_{=: T_2} \quad (140)$$

In the first term T_1 , applying the Cauchy-Schwartz,

$$T_1 \propto \mathbb{E}_{V,U} \int dy \mathbb{E}_{W \sim Q} \left(e^{-(y-\kappa g_U)^2/4} |g_W|^{jp} \right) \left(e^{-(y-\kappa g_U)^2/4} |\text{He}_j(y - \kappa g_U)|^p \right) \quad (141)$$

$$\leq \left(\mathbb{E}_V \int dy \mathbb{E}_U [e^{-(y-\kappa g_U)^2/2}] \mathbb{E}_{W \sim Q} [|g_W|^{2jp}] \right)^{1/2} \left(\mathbb{E}_V \int dy \mathbb{E}_U e^{-(y-\kappa g_U)^2/2} |\text{He}_j(y - \kappa g_U)|^{2p} \right)^{1/2} \quad (142)$$

$$= \left(\mathbb{E}_V \int dy \mathbb{E}_{W \sim \mathcal{N}(0,1)} [e^{-(y-\kappa g_W)^2/2} |g_W|^{2jp}] \right)^{1/2} \left(\int dy e^{-y^2/2} |\text{He}_j(y)|^{2p} \right)^{1/2} \quad (143)$$

$$= \left(\mathbb{E}_V \int dy e^{-y^2/2} \mathbb{E}_{W \sim \mathcal{N}(0,1)} [|g_W|^{2jp}] \right)^{1/2} \left(\int dy e^{-y^2/2} |\text{He}_j(y)|^{2p} \right)^{1/2} \quad (144)$$

$$= \left(\sqrt{2\pi} \mathbb{E}_{z \sim \mathcal{N}(0,1)} [|g(z)|^{2jp}] \right)^{1/2} \left(\int dy e^{-y^2/2} |\text{He}_j(y)|^{2p} \right)^{1/2} < \infty, \quad (145)$$

where the the first factor is bounded as $|g(x)| < C(1 + |x|^b)$, for some constants $C \in \mathbb{R}$, $b \in \mathbb{N}$ (Definition C.1). Moreover, we have used

$$\mathbb{E}_{V,W} [g_W^2] = \mathbb{E}_{W,V} [g^2(\sqrt{m}V + \sqrt{1-m}W)] = \mathbb{E}_z [g^2(z)]. \quad (146)$$

Similarly,

$$T_2 \propto \mathbb{E}_V \int dy \mathbb{E}_U \left[e^{-(y-\kappa g_U)^2/2} |\text{He}_j(y - \kappa g_U)|^p |g_U|^{jp} \right] \quad (147)$$

$$= (\mathbb{E}_{z \sim \mathcal{N}(0,1)} [|g(z)|^{jp}]) \left(\int dy e^{-y^2/2} |\text{He}_j(y)|^p \right) < \infty \quad (148)$$

Both T_1 and T_2 are bounded by quantities independent of κ and m , and that are functions of the finite moments $\mathbb{E}_z [g^k(z)]$, which completes the proof. \square